

https://dspace.org/

# The effect of microwave treatment on potassium promoted iron Fischer-Tropsch catalysts

**Dlamini, Mbongiseni William**

**2012-07-03**
http://hdl.handle.net/10539/11587

Downloaded from a DSpace repository. https://dspace.org/

# Chapter 5

# Microwave modification of silica-supported Fischer-Tropsch catalysts: The effect of potassium

## *5.1 Introduction*

Fischer-Tropsch synthesis (FTS) is a heterogeneous catalytic process for the transformation of synthesis gas ($CO + H_2$) into hydrocarbons. This process was first reported more than eighty years ago by two German chemists, Hans Fischer and Franz Tropsch.[1,2] Iron-based FTS catalysts provide both hydrogenation and water-gas-shift activities, imposing a flexible option for a typical coal-derived CO-rich syngas conversion process.[3,4] However, the use of conventional, precipitated Fe catalysts in the most economical reactors, slurry bubble columns, has been limited by their low structural integrity; i.e. unsupported, precipitated iron catalysts undergo attrition at high rates to fine particles (approximately micrometer diameter or smaller), leading to uneconomical loss of catalyst, high slurry viscosity, and difficulty in separating catalyst particles from the wax product.[5-10]

Supports can play a variety of roles in heterogeneous catalysis: 1) disperse the active phase giving a catalytically active phase with a high surface area; 2) stabilise the active phase against loss of surface area during the reaction; and 3) maintain the catalyst mechanical strength and 4) facilitate the mass or heat transfer in a diffusion-limited or an exothermic reaction.[11] $SiO_2$ has been studied extensively as a catalyst support for the FT reaction, and has been shown to be an excellent structural promoter for Fe based catalysts.[12-14]

Pre-treatment of iron catalysts has an important influence on the FTS activity and selectivity.[15] In the preceding chapter, it was shown that microwave pre-treatment

changes the surface properties of unsupported catalysts and these changes have been found to be dependent on the loading of potassium. Of course, it is desirable to understand why this phenomenon occurs. The objective of this work was to investigate the existence of a relationship between the microwave pre-treatment effect and the content of potassium in well-dispersed, silica-supported Fe catalysts. Effects due to the catalyst crystallite size and the pre-treatment time were also investigated.

## *5.2 Experimental*

Catalyst preparation was mainly done using the incipient wetness impregnation technique as explained in Chapter 3, and the catalyst compositions are tabulated in Table 5.1. For brevity, the catalyst labelling *x*K/10Fe/$SiO_2$ was used, where *x* is the weight percent of potassium in the sample. Microwave modified samples are denoted as *x*K/10Fe/$SiO_2$-MW. A 10% iron loading was maintained in all the samples. Techniques used in this study include XRF, TEM, EDS, BET, TPR, TPSR-MS and FTS. Further details on how these techniques were performed are discussed in Chapter 3. The effect of crystallite size on the microwave effect was also investigated by preparing smaller size crystallites using the deposition precipitation procedure.

## *5.3 Results and discussion*

The effects of microwave pre-treatment on the bulk properties of the catalysts were studied. In the latter sections of this chapter, the effect of microwave pre-treatment on the surface properties of the catalysts will be presented.

### 5.3.1 X-Ray fluorescence (XRF)

Elemental composition of the catalysts was confirmed using XRF. The actual and calculated weight loadings of potassium and iron in the catalyst are displayed in Table 5.1. For all the catalysts, the intended weight loading of iron was 10 wt. %. It is apparent from Table 5.1 that the calculated and the actual weight loadings of both iron and potassium are similar, indicating that reasonable accuracy was attained during catalyst preparation. For iron loadings, the maximum error between the calculated and the actual values confirmed by XRF was found to be 0.4 wt. %, while a 0.09 wt. % maximum error was found for potassium. The catalyst without any loaded potassium (0K/10Fe/$SiO_2$) was analysed twice to verify the precision of the instrument. A value of 10.1 wt. % for the Fe content was observed in both analyses. Variations between the calculated and the XRF determined values were taken to be due to catalyst preparation procedures.

**Table 5.1** Elemental compositions of the catalysts as determined by XRF.

| Catalyst | Fe loading (wt. %) | | K loading (wt. %) | |
|---|---|---|---|---|
| | **Calculated** | **Actual** | **Calculated** | **Actual** |
| 0K/10Fe/$SiO_2$ | 10.0 | 10.1 | 0.00 | 0.01 |
| 0.2K/10Fe/$SiO_2$ | 10.0 | 10.4 | 0.2 | 0.24 |
| 0.5/K10Fe/$SiO_2$ | 10.0 | 10.4 | 0.5 | 0.54 |
| 0.7K/10Fe/$SiO_2$ | 10.0 | 10.4 | 0.7 | 0.79 |
| 1.0K/10Fe/$SiO_2$ | 10.0 | 10.2 | 1.0 | 1.09 |
| 1.5K/10Fe/$SiO_2$ | 10.0 | 10.0 | 1.5 | 1.59 |
| 0K/10Fe/$SiO_2$ | 10.0* | 10.1* | 0.0* | 0.01* |

* This sample analysis was repeated to verify the precision of the instrument

## 5.3.2 Transmission electron microscopy (TEM)

The morphology and particle size of the crystallites was analysed using TEM. Figure 5.1 shows typical images of (a) 0.2K/10Fe/$SiO_2$ and (b) 0.7K/10Fe/$SiO_2$ catalysts. TEM results for the other samples are shown in the Appendix. In these images iron particles are seen as dark spheres while the silica support is much lighter in colour. Energy dispersive X-ray spectroscopy (EDS) was used to confirm the identity of the particles. Figure 5.2 shows an EDS spectrum confirming the presence of both iron and silica in the catalyst. An EDS spectrum of the silica alone is displayed in Appendix B. In both spectra a copper signal is observed since copper grids were used to suspend the samples. Potassium peaks were not detected in any of the catalysts, which could indicate that the potassium was evenly distributed throughout the sample. From the TEM images it can be noted that the iron crystallites were also well dispersed on the silica support. The average particle size for the non-microwaved iron particles was found to be in the range 40 – 60 nm for the various loadings of potassium. Microwave pre-treatment did not alter the morphology or the particle sizes of the catalysts since similar data was recorded for both the microwaved and the non-microwaved samples.

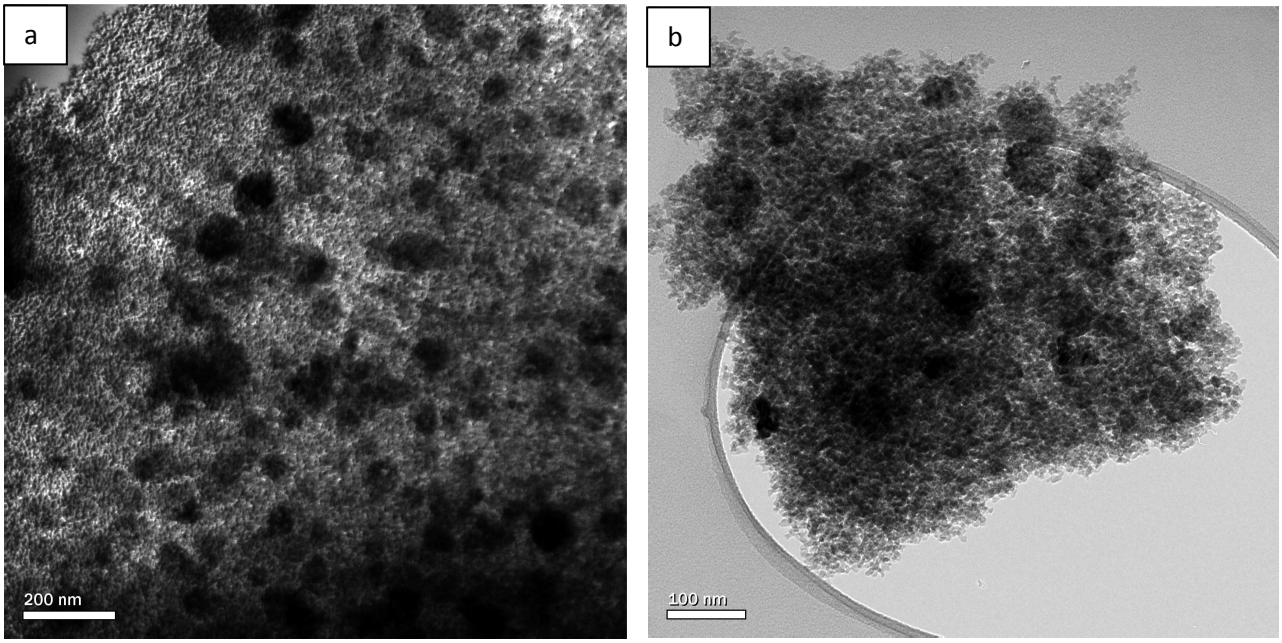



**Figure 5.1** TEM images of 0.2K/10Fe/$SiO_2$ and 0.7K/10Fe/$SiO_2$ catalysts.

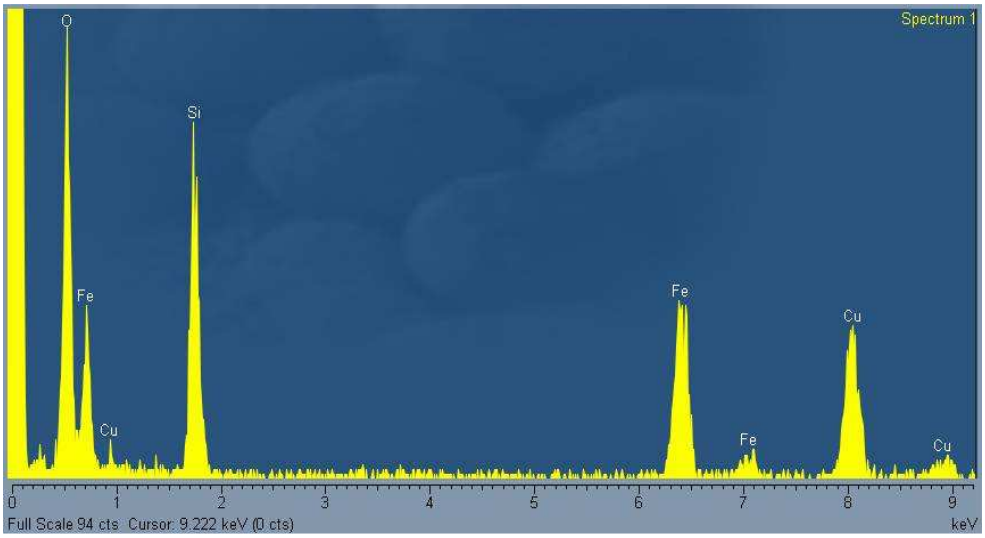



**Figure 5.2** A typical EDS spectrum of a K/Fe/$SiO_2$ catalyst confirming the presence of iron.

## 5.3.3 BET analysis by $N_2$ physisorption

The determination of surface area is considered to be an important requirement in the characterization of a catalyst, although the catalytic activity may only be indirectly related to the total surface area. In addition, it is usually necessary to specify the pore content and pore structure since these parameters may control the transport of the reactants and products in a catalytic reaction.[16]

Table 5.2 summarizes the surface area and pore volume measurements of the different catalysts, prior to and after exposure to microwave radiation for 10 seconds. A maximum error of ± 2% is associated with these values. The BET surface areas of all the silica-supported catalysts are in the range of 220 – 284 $m^2/g$. By comparing the BET surface areas of the catalysts with varying loadings of potassium, it is observed that catalysts with higher loadings of potassium have lower BET surface areas (see Figure 5.3). The study of Dry and Oosthuizen[17] over a fused iron catalyst also gave similar results: as more alkali was added, the greater the loss in surface area. These findings were ascribed to the fact that potassium could improve the agglomeration of

the FeOOH precursor and could further enlarge the crystallite size of $\alpha$-$Fe_2O_3$ after calcination, which would induce the decrease in surface area.

The pore volume of these catalysts decreases marginally in a similar way to that observed for the surface area. The unpromoted catalyst has the highest surface area and pore volume while the catalyst with the highest loading of the promoter shows the lowest surface area and pore volume.

The catalysts were then pre-treated with microwave radiation at a 450 W power level for 10 seconds. The results obtained are shown in Table 5.2 and Figure 5.3. The surface areas were found to decrease with an increase in the content of potassium in the catalysts as was observed in non-microwaved samples. The data shown in Figure 5.3 illustrates that the loss of surface area with potassium is similar in both microwaved and non-microwaved samples. This suggests that microwave pre-treatment does not affect the textural properties of the catalysts.

**Table 5.2** Textural properties of the silica supported catalysts before and after microwave pre-treatment.

| **Catalyst composition (wt. %)** | **BET surface area ($m^2$/g)** | | **Pore volume ($cm^3$/g)** | |
|---|---|---|---|---|
| | A | B | A | B |
| 10 $Fe/SiO_2$ | 281 | 284 | 0.88 | 0.85 |
| 0.2 K/10 $Fe/SiO_2$ | 256 | 252 | 0.86 | 0.87 |
| 0.5 K/10 $Fe/SiO_2$ | 255 | 254 | 0.87 | 0.86 |
| 0.7 K/10 $Fe/SiO_2$ | 235 | 237 | 0.85 | 0.85 |
| 1.0 K/10 $Fe/SiO_2$ | 231 | 233 | 0.85 | 0.84 |
| 1.5 K/10 $Fe/SiO_2$ | 221 | 220 | 0.85 | 0.84 |

A = Without any microwave exposure; B = After 10 seconds of microwave pre-treatment (450 W power level)

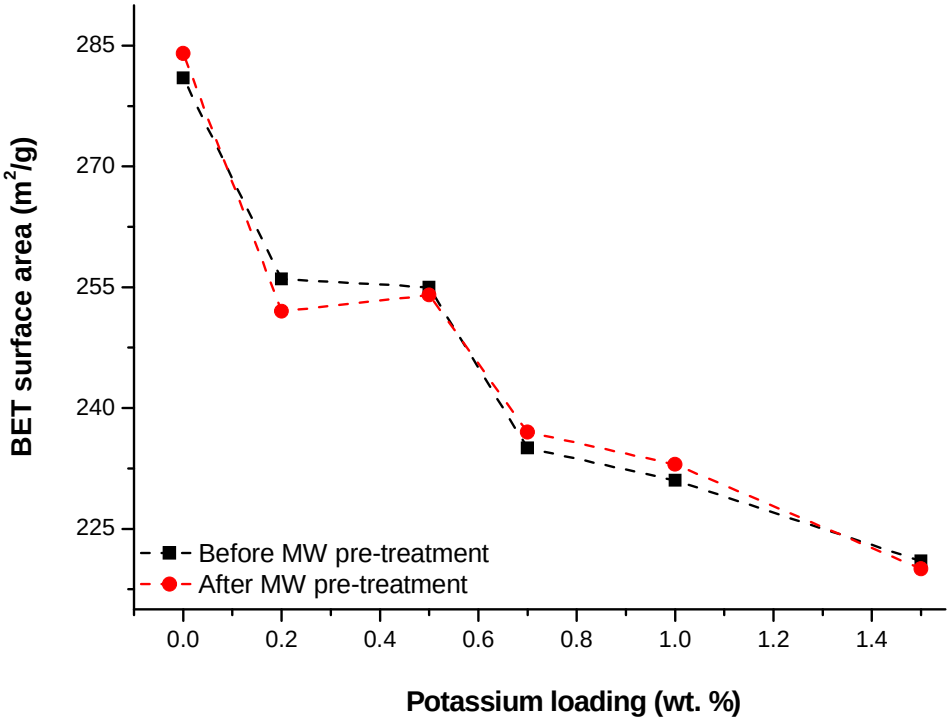



**Figure 5.3** BET surface areas of microwave pre-treated and non- pre-treated catalysts of different loadings of potassium.

## 5.3.4 Temperature programmed reduction (TPR)

The catalysts with different potassium loadings were further characterized using $H_2$-TPR prior to microwave pre-treatment. The hydrogen consumption profiles obtained as a function of temperature are displayed in Figure 5.4. Data from this figure is tabulated in Table 5.3. While the reduction of unsupported iron catalysts occurs in two simple steps, a more complex behaviour is exhibited by silica supported samples. In unsupported catalysts the two steps represent the reduction of α-$Fe_2O_3$ to $Fe_3O_4$ and then further reduction of $Fe_3O_4$ to α-Fe.[18]

At a low promoter loading (0.2 wt. % K) the profile shows four reduction peaks. The small peak at 310 $^oC$ could be related to a minor process of reduction of small

particles of $Fe_2O_3$ occurring at the surface i.e. at temperatures lower than 390 $^oC$. This peak increases in intensity and also shifts to higher temperatures as the loading of potassium is increased in the samples. Also, at potassium loadings of 0.7, 1.0 and 1.5 wt. % K the peak gradually separated to two distinct peaks. The second reduction peak for the 0.2K/10Fe/$SiO_2$ catalyst occurs at 425 $^oC$ and it represents the reduction of bulk $Fe_2O_3$ to $Fe_3O_4$. Corresponding peaks in the other samples at higher promoter contents have been highlighted using a dotted line. Clearly the peak shifts to higher temperatures with an increase in the potassium loading. This is because potassium inhibits the reducibility of iron.[19] In contrast to Peak 1, this peak decreases in intensity for samples with higher potassium contents. This observation is consistent with the assignment of Peak 1.

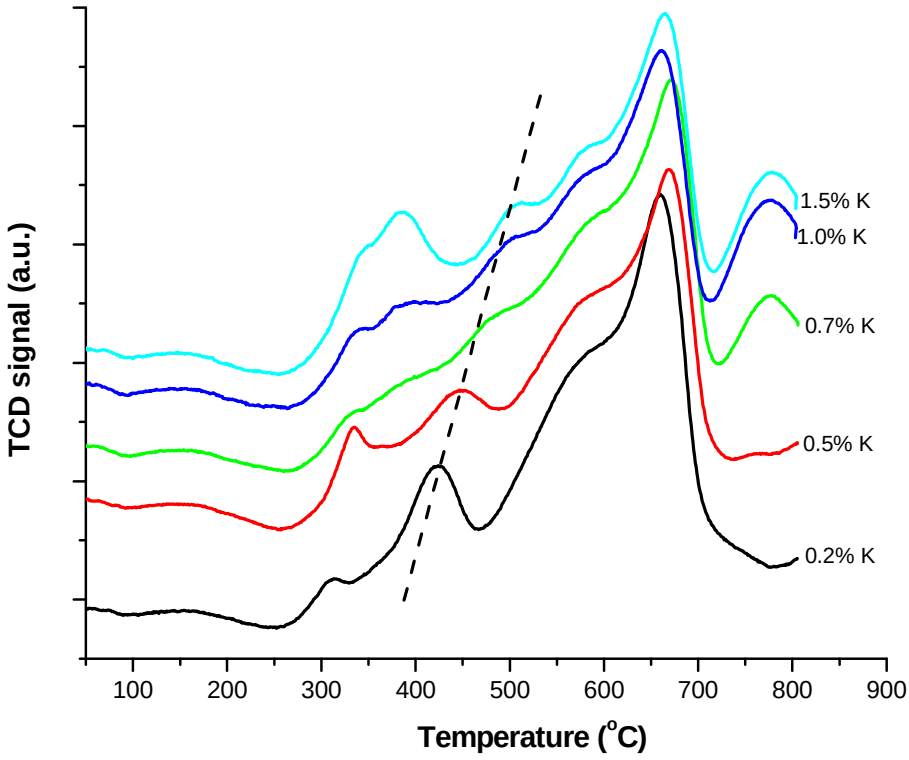



**Figure 5.4** $H_2$-TPR profiles for the catalysts of the composition *x*K/10Fe/$SiO_2$, *x* varies from 0 to 1.5 wt. %.

**Table 5.3** Reduction temperatures for the various silica supported catalysts.

| Catalyst | Reduction temperatures ($^oC$) | | | |
|---|---|---|---|---|
| | **Peak 1** | **Peak 2** | **Peak 3** | **Peak 4** |
| 0.2K/10Fe/$SiO_2$ | 310 | 425 | 577 | 657 |
| 0.5 K/10Fe/$SiO_2$ | 333 | 448 | 583 | 669 |
| 0.7 K/10Fe/$SiO_2$ | 335/389 | 479 | 586 | 672 |
| 1.0 K/10Fe/$SiO_2$ | 341/390 | 505 | 578 | 660 |
| 1.5 K/10Fe/$SiO_2$ | 341/385 | 505 | 581 | 663 |

The reduction of $Fe_3O_4$ to Fe occurs at 577 $^oC$ for the 0.2K/10Fe/$SiO_2$ sample and is labelled as Peak 3. This peak does not shift with the addition of potassium. Peak 4 occurs between 657 and 663 $^oC$ for the various samples as tabulated in Table 5.3. This peak represents the reduction of iron(II)silicate to α-Fe. This peak is broad and it indicates that large amounts of iron silicates were present in the samples. The large amounts of iron silicates are attributed to strong interaction between the iron species and silica. A rather small peak at ~750 $^oC$ is also observed. It could be assigned to the reduction of the $K_2CO_3$ phase, in agreement with its growth with the increase of the potassium content and the analogous assignment of Stobe *et al.*[20] and Guglielminotti and co-workers.[21] Microwave pre-treatment did not introduce any significant changes in the reduction profiles of the silica supported catalysts since similar data was recorded before and after microwave modification.

## 5.3.5 Temperature programmed surface reaction-mass spectrometry (TPSR-MS)

### 5.3.5.1 Blank run

In this study, CO was adsorbed on pre-reduced K/Fe/$SiO_2$–type catalysts. Catalyst reduction was performed for 6 hours at 350 $^oC$. CO adsorption was then done for an hour. The adsorbed species were subsequently hydrogenated with $H_2$ at a flow rate of 20 ml/min to give hydrocarbons. Data in Figure 5.5 shows typical profiles obtained during the TPSR experiment. One profile shows the rate of formation for hydrocarbons as monitored using a flame ionisation detector (FID), while the other profile shows the rate of methane formation which was monitored using a quadrupole mass spectrometer (QMS). From this figure it can be noted that the FID and the QMS signals are similar, indicating that methane is the main hydrocarbon produced during the hydrogenation of previously adsorbed CO species. Higher hydrocarbons (ethane, propane, etc.) were not detected during these experiments. This is quite reasonable considering the very high $H_2$/CO ratio on the surface of the catalyst during this experiment. The total amount of methane produced was calculated by measuring the total peak area under the TPSR profile and the use of methane calibration curves (see Chapter 3). Therefore, using constant flow conditions, the FID detector output can be taken to be proportional to the rate of the reaction. The peak intensity is proportional to the rate of formation of methane at a particular temperature.

Two methane signals are observed in Figure 5.5. These peaks indicate that there are two kinds of CO adsorption sites on the surface of the catalyst. The observed peaks are broad, suggesting that several overlapping peaks co-exist. The peaks have been de-convoluted and studies on this procedure are discussed in the next sections.

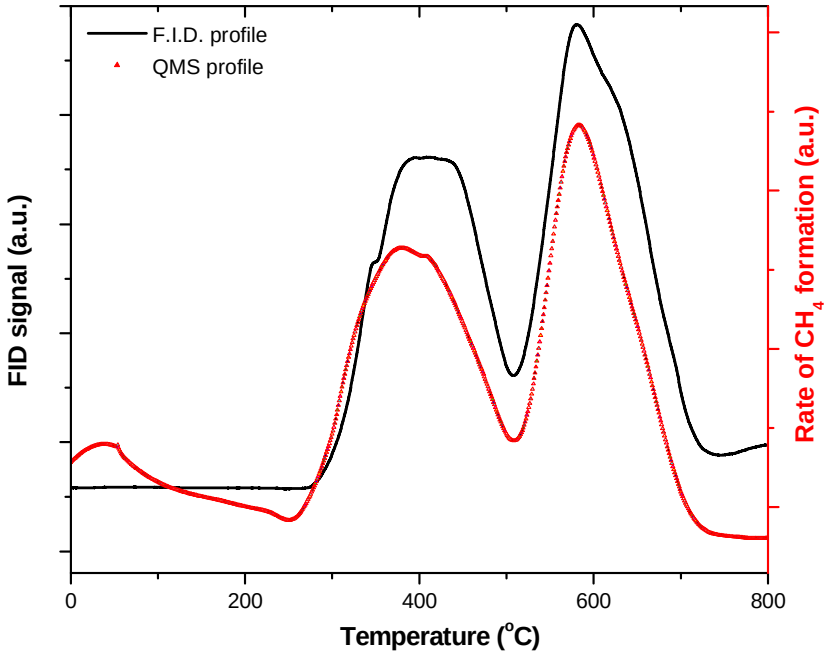



**Figure 5.5** A comparison of typical TPSR profiles obtained from an FID (─) and a QMS (─) that were performed simultaneously when using a silica-supported catalyst.

### 5.3.5.2 The effect of potassium

Figure 5.6 shows TPSR profiles of catalysts with varying loadings of potassium (0 to 1.5 wt. % K) as monitored using a gas chromatograph (GC) fitted with a flame ionization detector (FID) to detect species evolving as a function of temperature. As was shown in the preceding section, methane was the main hydrocarbon detected during TPSR experiments. The $CH_4$ profiles shown in the figure look similar in shape i.e. two sets of peaks appearing at ~300 $^o$C and at ~500 $^o$C are common in the profiles. The peaks shift to higher temperatures as the loading of potassium is increased. It is known that $K_2O$ on the surface of an iron catalyst increases the Fe–C bond strength for CO bonded to Fe,[22] hence leading to the shift to higher peak temperatures with K loading. Graf and Muhler[23] reached the same conclusion on the influence of the potassium promoter after performing CO temperature programmed desorption (TPD) experiments. The peaks recorded in this work are broad and this indicates the existence of several overlapping peaks that coexist. These signals were deconvoluted by fitting Gaussian curves.

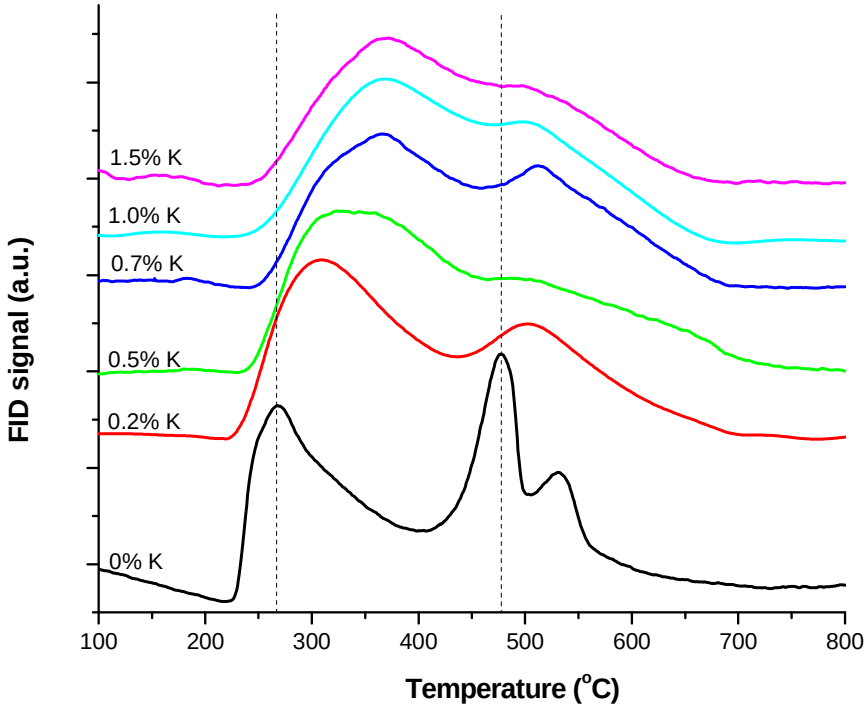



**Figure 5.6** TPSR profiles of *x* K/10Fe/$SiO_2$-type catalysts, *x* varies from 0 to 1.5 wt. %.

The total areas under these peaks were obtained by integration and were used together with methane calibration data to quantify the $CH_4$ evolved during the TPSR experiments. The total amounts of methane evolved from the various catalysts are listed in Table 5.4 as a function of the potassium content. The $CH_4$ produced from all the catalysts is in the range 31–32 µmol $g^{-1}$. From this table it is evident that the potassium loading does not have a significant impact on the amount of methane produced over these catalysts. This implies that surface iron crystallites are not affected by the potassium ions. The data shown in Table 5.4 was also used to ascertain the reproducibility of the results obtained from the TPSR technique. From the results obtained it can be appreciated that all the samples analysed varied by 1 µmol $g^{-1}$ $CH_4$, which shows that the data recorded from this technique is reproducible. Despite the different loadings of potassium in the samples, the results were still conclusive since all the samples were not microwaved. It was noted that even though potassium did not affect the total $CH_4$ evolved, it did change the surface carbon species from which $CH_4$ is then produced. For example adsorbed atomic carbon ($C_\alpha$) formation decreased monotonously as the loading of potassium was increased.

**Table 5.4** Peak parameters and the total amount of $CH_4$ produced from the catalysts.

| Catalyst | Peak parameters | | | | Total $CH_4$ evolved ($\mu mol\ g^{-1}$) |
|---|---|---|---|---|---|
| | Carbidic α | amorphous β | carbide γ | graphitic δ | |
| 0K/Fe/$SiO_2$ | 22.2/268 | 31.9/339 | 33.3/474 | 12.6/535 | 31 |
| 0.2K/10Fe/$SiO_2$ | 18.9/288 | 35.5/348 | 16.7/493 | 28.9/528 | 32 |
| 0.5K/10Fe/$SiO_2$ | 12.7/296 | 35.4/357 | 29.6/468 | 22.3/594 | 32 |
| 0.7K/10Fe/$SiO_2$ | 14.1/314 | 39.4/381 | 35.6/507 | 10.9/601 | 31 |
| 1.0K/10Fe/$SiO_2$ | 9.4/328 | 55.7/386 | 26.5/512 | 8.4/594 | 32 |
| 1.5K/10Fe/$SiO_2$ | 7.0/304 | 32.1/360 | 36.1/439 | 24.8/540 | 31 |

### 5.3.5.3 The microwave pre-treatment effect

Solid-state modification of the catalysts using microwave radiation was done for 10 seconds using a power level of 450 W. Prior to pre-treatment, the catalysts were evenly dispersed in a microwave-transparent Pyrex watch glass. The microwave pre-treatment effect was investigated as a function of the loading of potassium in the catalysts. The effect of microwave pre-treatment on the supported catalysts is illustrated in Figure 5.7. From this plot it can be noted that the profiles obtained after microwave pre-treatment differ from the non-microwaved samples which gave similar profiles independent of the promoter loading (see Figure 5.6). Four $CH_4$ peaks could be detected upon fitting Gaussian curves to these profiles. This suggests that there are four different active sites of iron that bond to the CO during the adsorption process. These different iron sites lead to four different Fe–C interactions and the four C atoms are assigned as α, β, γ and δ-carbons in this work. Correspondingly, these carbon

species are designated to be due to adsorbed atomic carbon, amorphous surface methylene chains or films, bulk iron carbide, and graphitic carbon.[24,25] The contributions of these carbon species to the total hydrocarbon content have been compared. The comparison was also made between microwaved and non-microwaved samples of similar promoter contents as shown in the tables and figures given below.

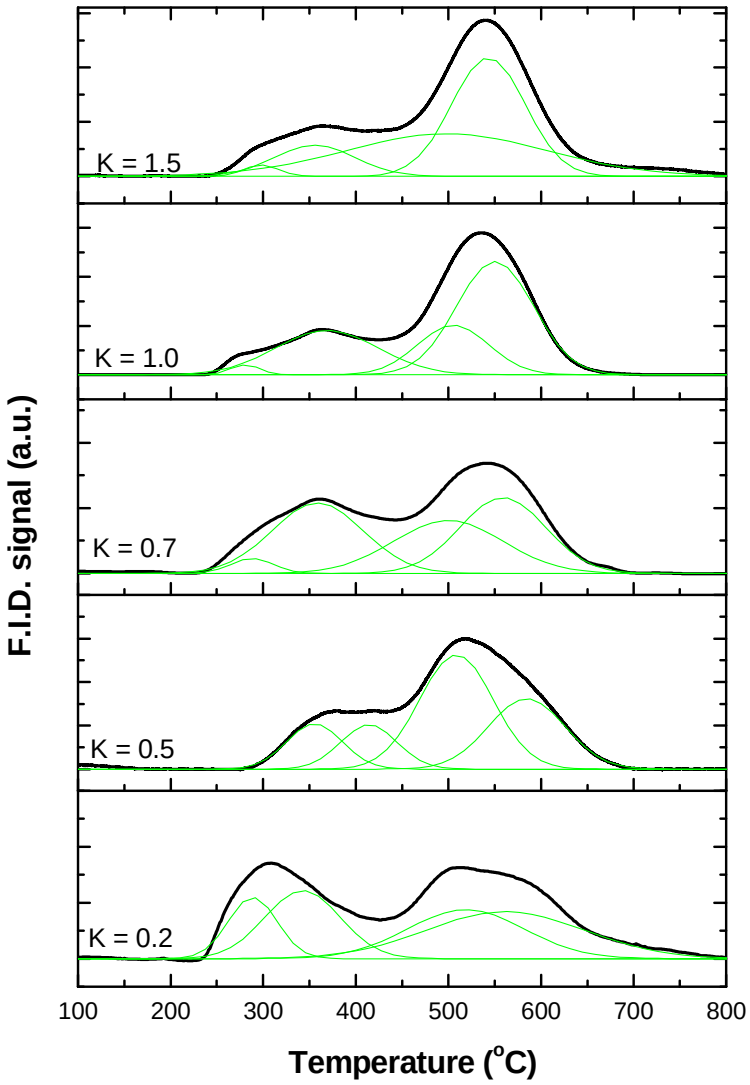



**Figure 5.7** The effect of microwave pre-treatment on supported FT catalysts with varying promoter loadings.

Figure 5.8 shows TPSR profiles for 0.2K/10Fe/$SiO_2$ (not modified) and 0.2K/10Fe/$SiO_2$-MW (modified using microwave radiation) catalysts displaying the evolution of methane as a function of temperature. Data on the individual contributions of the carbon species is tabulated in Table 5.5. From the data in Table 5.5 and Figure 5.8 it is evident that microwave pre-treatment at this loading of potassium induces a small increase in the overall $CH_4$ evolved. The total area for the $CH_4$ peaks in the 0.2K/10Fe/$SiO_2$-MW catalyst corresponds to 36 µmol $g^{-1}$, whereas 32 µmol $g^{-1}$ $CH_4$ was evolved from the 0.2K/10Fe/$SiO_2$ catalyst. This increase in the $CH_4$ content is equivalent to 13%, which is induced by the microwave pre-treatment effect. An analysis of the contributions from the various carbon species shows that the α- and the β-carbon species appearing at 289 and 344 $^oC$, respectively, decreases after microwave pre-treatment. However, Figure 5.8b and Table 5.5 shows that $CH_4$ formation in the microwaved sample is severely enhanced from the γ- and δ-carbon species. As a result the γ- and the δ- species contribute a combined 61% of the 36 µmol $g^{-1}$ produced from the 0.2K/10Fe/$SiO_2$-MW catalyst.

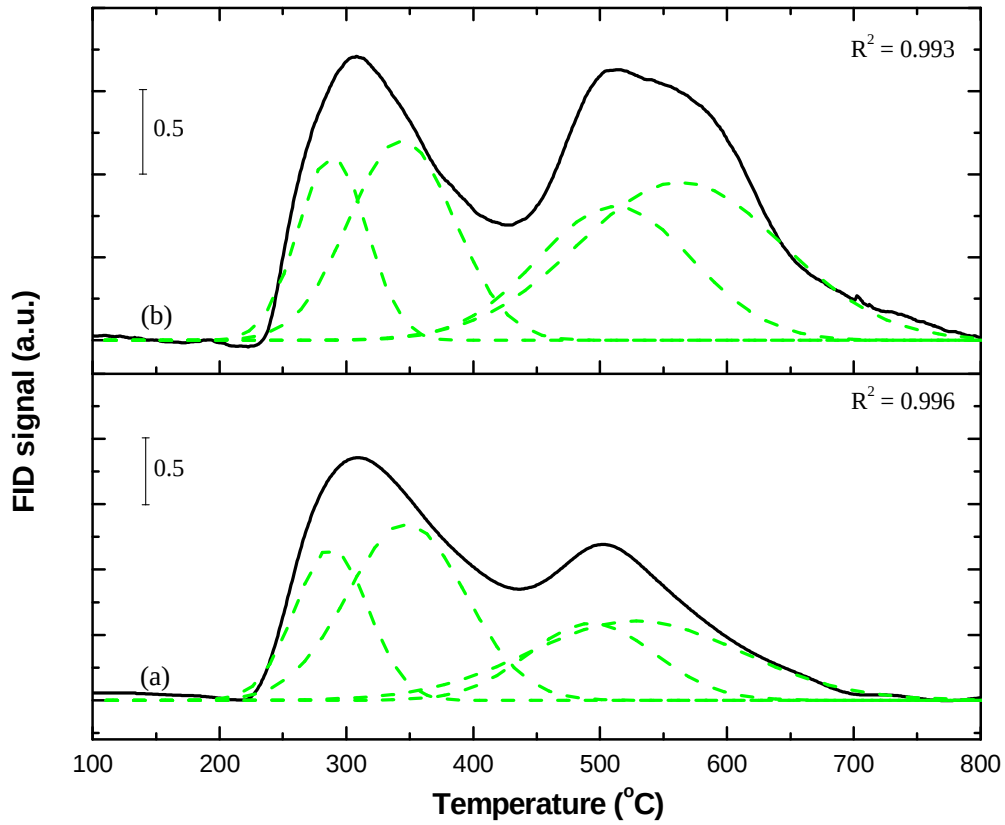



**Figure 5.8** TPSR profiles of (a) 0.2K/10Fe/$SiO_2$ and (b) 0.2K/10Fe/$SiO_2$-MW catalysts. Pre-treatment conditions: 10 seconds, 450 W.

Upon increasing the loading of potassium from 0.2 wt. % to 0.7 wt. % in the samples, a significant change in the TPSR profile for the microwave modified catalyst was noted. The methanation plots obtained from 0.7K/10Fe/$SiO_2$ and the 0.7K/10Fe/$SiO_2$-MW catalyst are displayed in Figure 5.9a and Figure 5.9b respectively. Peak parameters for the individual carbon species and details for the total $CH_4$ evolved are listed in Table 5.5. The microwaved catalyst displays an overall increase in the rate of methanation of 23% relative to the non-microwaved catalyst. This increase in methane production is attributed to the microwave pre-treatment effect as all other parameters were kept constant. Figure 5.9b shows that the change in the profile is due to $CH_4$ produced from δ-carbon species at 559 $^oC$ which increases considerably. Microwave pre-treatment results in slight decreases in the contributions from adsorbed atomic

carbon ($C_\alpha$), surface methylene chains ($C_\beta$) and bulk iron carbide ($C_\gamma$) species at 0.7 wt. % K.

**Table 5.5** Peak parameters of individual carbon species and total $CH_4$ peak areas from the TPSR profiles of 0.2K/10Fe/$SiO_2$, 0.5K/10Fe/$SiO_2$, 0.7K/10Fe/$SiO_2$, 1.0K/10Fe/$SiO_2$ and 1.5K/10Fe/$SiO_2$-MW catalysts prior and after microwave pre-treatment.

| Catalyst | Peak parameters | | | | $CH_4$ total area ($\mu$mol $g^{-1}$) |
|---|---|---|---|---|---|
| | Carbidic α | amorphous β | carbide γ | graphitic δ | |
| 0.2K/10Fe/$SiO_2$ | 18.9/288 | 35.5/348 | 16.7/493 | 28.9/528 | 32 |
| 0.2K/10Fe/$SiO_2$-MW | 14.5/289 | 24.2/344 | 23.9/511 | 37.4/563 | 36 |
| 0.5K/10Fe/$SiO_2$ | 12.7/296 | 35.4/357 | 29.6/468 | 22.3/594 | 32 |
| 0.5K/10Fe/$SiO_2$-MW | 12.7/354 | 13.8/413 | 46.2/509 | 27.3/586 | 40 |
| 0.7K/10Fe/$SiO_2$ | 14.1/314 | 39.4/381 | 35.6/507 | 10.9/601 | 31 |
| 0.7K/10Fe/$SiO_2$-MW | 3.8/288 | 32.1/359 | 31.3/500 | 32.8/559 | 40 |
| 1.0K/10Fe/$SiO_2$ | 9.4/328 | 55.7/386 | 26.5/512 | 8.4/594 | 32 |
| 1.0K/10Fe/$SiO_2$-MW | 1.6/280 | 26.2/368 | 27.2/510 | 45.0/553 | 53 |
| 1.5K/10Fe/$SiO_2$ | 7.0/304 | 32.1/360 | 36.1/439 | 24.8/540 | 31 |
| 1.5K/10Fe/$SiO_2$-MW | 3.6/297 | 16.1/358 | 8.0/426 | 72.3/541 | 51 |

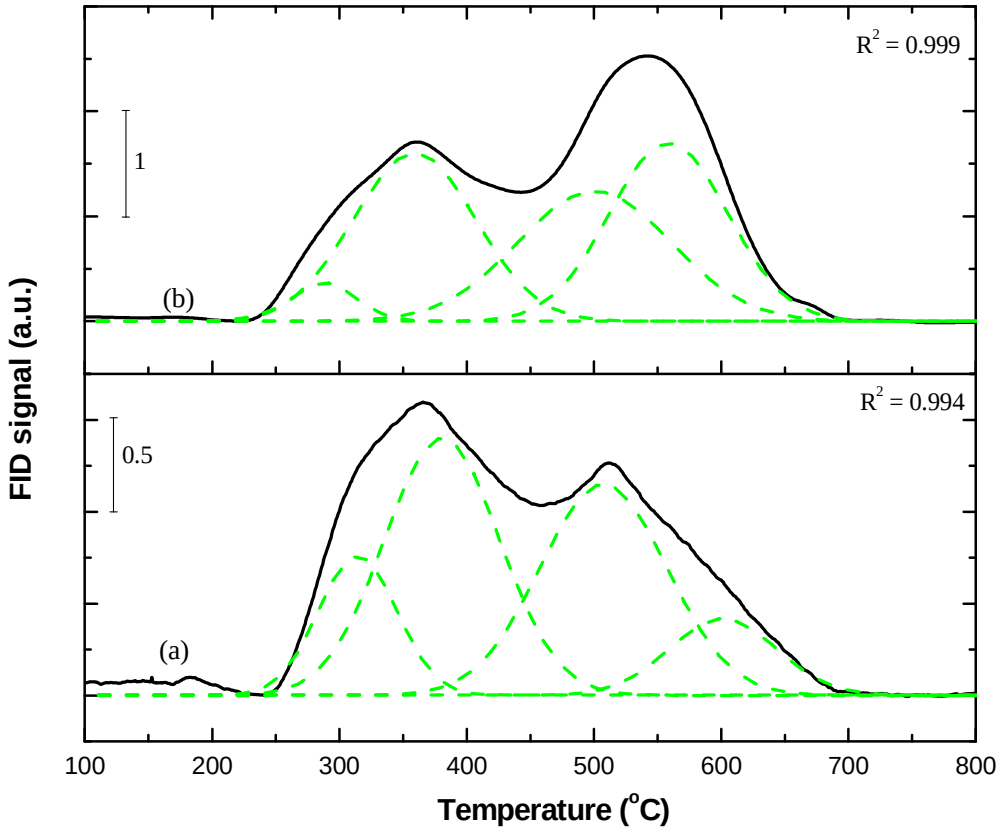



**Figure 5.9** TPSR profiles for 0.7K/10Fe/$SiO_2$ and 0.7K/10Fe/$SiO_2$-MW catalysts. Microwave pre-treatment conditions: 10 seconds duration, 450 W power level.

Figure 5.10 and Figure 5.11 displays TPSR profiles for the 1.0K/10Fe/$SiO_2$ and the 1.5K/10Fe/$SiO_2$ catalysts that were modified using microwave radiation and those that were not. Contributions from the various carbon species generated from these catalysts are shown in Table 5.6. The TPSR profiles for the modified catalysts (1.0K/10Fe/$SiO_2$-MW and 1.5K/10Fe/$SiO_2$-MW) clearly differ when compared to those recorded on the un-modified catalysts. Both these catalysts display a huge signal at around 540 $^oC$ which is due to $CH_4$ formed from carbide and graphitic carbon. These signals account for a combined 72% and 80% of the total hydrocarbons produced from the 1.0K/10Fe/$SiO_2$-MW and 1.5K/10Fe/$SiO_2$-MW catalysts. This is to be compared with the 35% and 61% combined contributions from carbide and graphite-like carbons recorded from the non-microwaved catalysts of the same

composition. The total methane evolved when using the 1.0K/10Fe/$SiO_2$-MW catalyst was 53 µmol $g^{-1}$, which shows a 66% $CH_4$ increase relative to the 1.0K/10Fe/$SiO_2$ catalyst which only produced 32 µmol $g^{-1}$. An increase of 64% was induced by microwave pre-treatment for the catalysts with 1.5 wt. % potassium. Methanation from the α- and β-carbon species was found to decrease after modification of both the 1.0 and 1.5 wt. % K samples, hence the decline in their percentage contribution to the total $CH_4$ evolved.

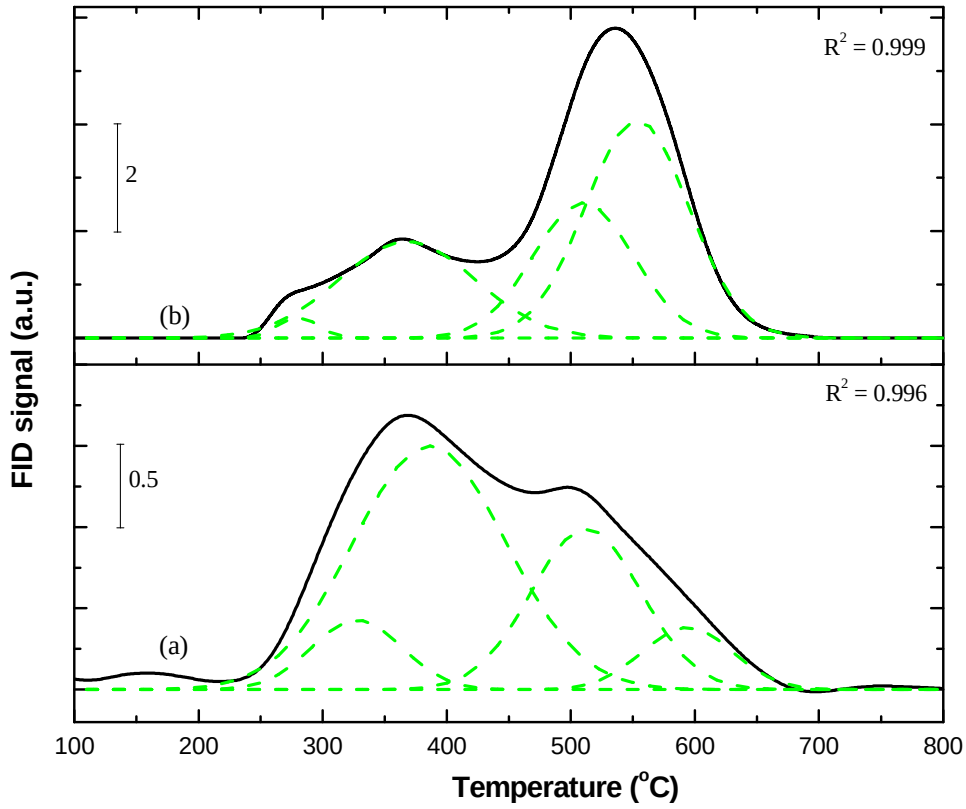



**Figure 5.10** TPSR profiles of 1.0K/10Fe/$SiO_2$ before and after microwave (MW) pre-treatment. Pre-treatment conditions: 10 seconds, 450 W.

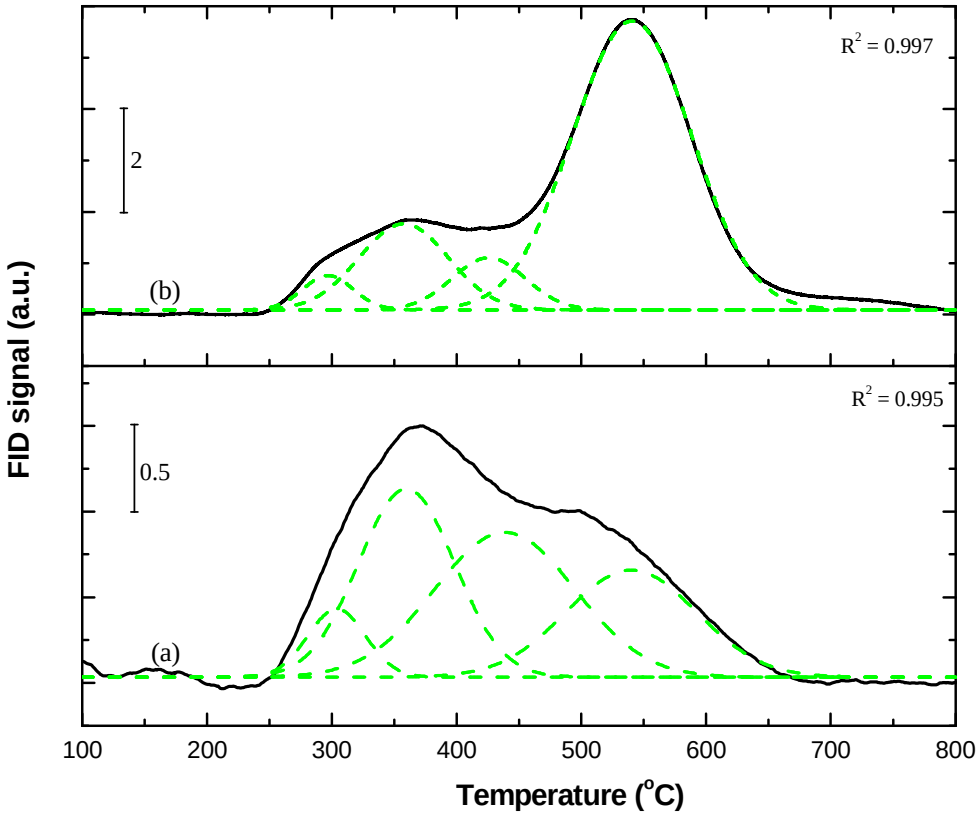



**Figure 5.11** TPSR profiles of 1.5 K/10 Fe/$SiO_2$ before and after microwave (MW) pre-treatment. Pre-treatment conditions: 10 seconds, 450 W.

A comparison of the total hydrocarbon content produced in both the microwaved and the non-microwaved catalysts during TPSR experiments is shown in Figure 5.12, as a function of the potassium loading. Clearly the increases seen were induced by microwave pre-treatment since all other variables were kept constant when catalysts of the same potassium loading were analysed. From this plot it can be seen that the microwave pre-treatment effect increases with the loading of potassium and attains an optimum value at 1.0 wt. % potassium loading where an increase of 66% in the total hydrocarbon content is attained. At low K loadings, microwave induced effects were seen to promote mainly methanation from γ- and δ-carbon species, while α- and β-carbon formation decreased. At high K loading, methanation from the α-, β- and γ-species was noted to decline after microwave pre-treatment. In contrast, $CH_4$

produced from graphitic carbon increases upon MW exposure. Un-modified catalysts display the opposite behaviour since methanation is generally favoured from α- and β-carbon species.

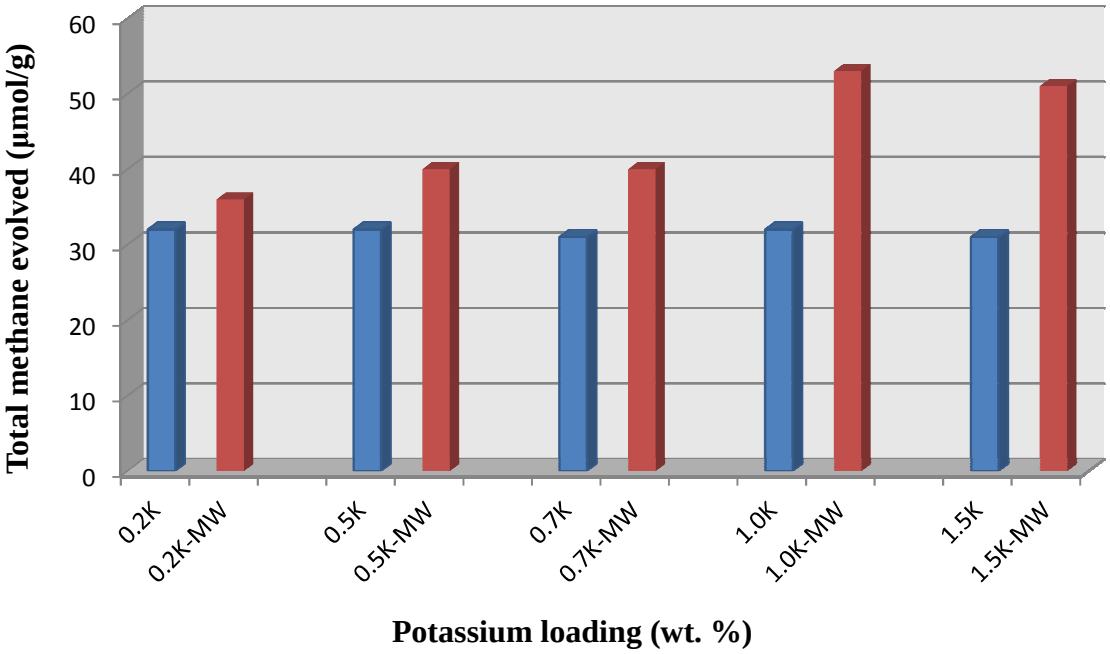



**Figure 5.12** Comparisons of methane formed in microwaved and non-microwaved samples as a function of potassium loading. All the catalysts are supported on silica and they contain 10 wt. % Fe.

The general increase in microwave-induced effects as a function of potassium can be explained by considering the known effects of potassium in Fischer-Tropsch synthesis. Without iron atoms it is difficult to cleave the C–O bond. The addition of K is done to further enhance this effect. The effect of microwave pre-treatment on a catalysts is believed to result in the migration of potassium ions to the surface of the catalyst.[26] Thus surface iron atoms in a microwave modified catalyst are surrounded by potassium ions and become "electron rich". The C–O bond on such iron atoms is easily cleaved and more hydrocarbons are produced. Linganiso[26] has shown using SIMS studies that microwave pre-treatment results in the migration of potassium ions to the surface of a catalyst hence increasing its activity.

The observed increase in $CH_4$ produced from graphitic-like carbon species upon microwave exposure is consistent with the explanation that potassium ions migrate to the surface of the catalyst during pre-treatment. It is well known that surface basicity can promote CO adsorption and suppress $H_2$ adsorption.[27]

### 5.3.5.4 The effect of the MW irradiation time

The microwave pre-treatment effect reported thus far has been accomplished by exposing the catalyst to microwave radiation that is at 450 W power level for only 10 seconds. To investigate the effect of the pre-treatment time, catalysts with 1.0 wt. % potassium loading were studied using both temperature programmed reduction (TPR) and temperature programmed surface reaction (TPSR). TPR was performed to investigate whether the period of MW pre-treatment affects the reducibility (a bulk property) of the catalyst, while TPSR was used to study any effects that the irradiation time may have on the surface properties of the catalyst. Earlier studies showed that the 1.0 wt. % loading was optimal for the microwave pre-treatment effect, and hence it was used in these investigations.

### 5.3.5.3.1 Temperature programmed reduction

The reduction profiles of iron catalysts that were irradiated for varying periods with microwaves are displayed in Figure 5.13. The temperatures at which the different reduction stages occur are listed in Table 5.6. The reduction behaviour of the non-microwaved sample was discussed in detail in section 5.3.4 where the four peaks (that are observed here) were assigned. MW pre-treatment was found not to change the general reduction profile of the catalyst. As illustrated in the table, the peaks from the microwaved samples show a marginal shift to lower temperatures. This indicates that MW pre-treatment could be used to enhance the reducibility of a catalyst. However, increased irradiation time does not affect the reduction behaviour of the catalyst as the profiles obtained after 40 seconds of microwave pre-treatment are similar to those recorded after 20 seconds.

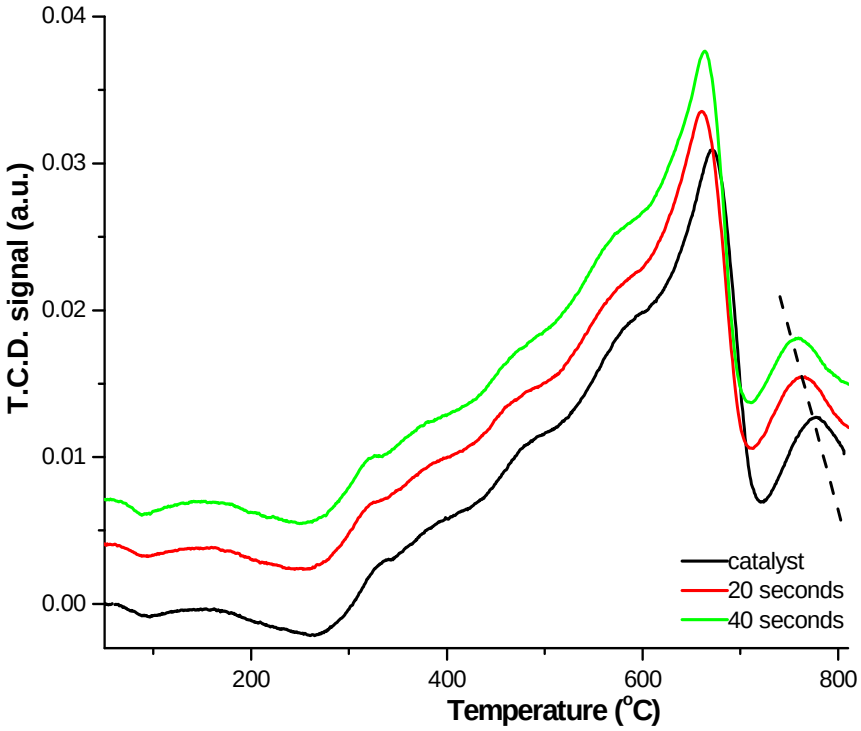



**Figure 5.13** TPR profiles for a 1.0K/10Fe/$SiO_2$ catalyst that was microwave pre-treated for varying periods.

**Table 5.6** TPR reduction temperatures obtained from Figure 5.13.

| **MW irradiation time** | **Reduction temperatures (°C)** | | | |
|---|---|---|---|---|
| | **Peak 1** | **Peak 2** | **Peak 3** | **Peak 4** |
| 0 seconds | 335/389 | 479 | 586 | 672 |
| 20 seconds | 325/382 | 466 | 571 | 660 |
| 40 seconds | 323/378 | 472 | 575 | 661 |

### 5.3.5.4.2 Temperature programmed surface reaction

TPSR profiles acquired during the investigation of the effect of the MW irradiation time followed the general pattern as discussed in section 5.3.5.3 with the profiles displaying two broad peaks before de-convolution (see Appendix C). Tabulated in Table 5.7 are the values of the total methane evolved during the TPSR experiments for the 1.0K/10Fe/$SiO_2$ catalyst that was irradiated for varying periods using microwaves. It can be seen from this table that the total methane produced increases as the microwave irradiation time is increased from 0 seconds (without any pre-treatment) to 10 minutes.

**Table 5.7** Total methane produced on the TPSR experiments using the 1.0K/10Fe/$SiO_2$ catalyst that was microwave pre-treated for varying periods.

| **Microwave pre-treatment time** | **Total $CH_4$ evolved (μmol $g^{-1}$)** |
|---|---|
| 0 seconds | 32 |
| 10 seconds | 53 |
| 20 seconds | 50 |
| 30 seconds | 59 |
| 40 seconds | 57 |
| 2 minutes | 188 |
| 5 minutes | 194 |
| 10 minutes | 232 |

To identify the origin of the increases in methane production after microwave pre-treatment, a plot of the $CH_4$ from the two broad peaks is shown in Figure 5.14. As seen in preceding sections, the low temperature broad peak accounts mainly for methane produced from α- and β-carbon species, while the high temperature broad peak accounts for methane evolved from γ- and δ-carbon species. As illustrated by this figure, the broad low temperature peak area is fairly constant throughout the

irradiation period. It is not affected by the irradiation time. On the contrary, the high temperature peaks displays significant increases as the irradiation time is increased, especially between 50 and 100 seconds of MW irradiation.

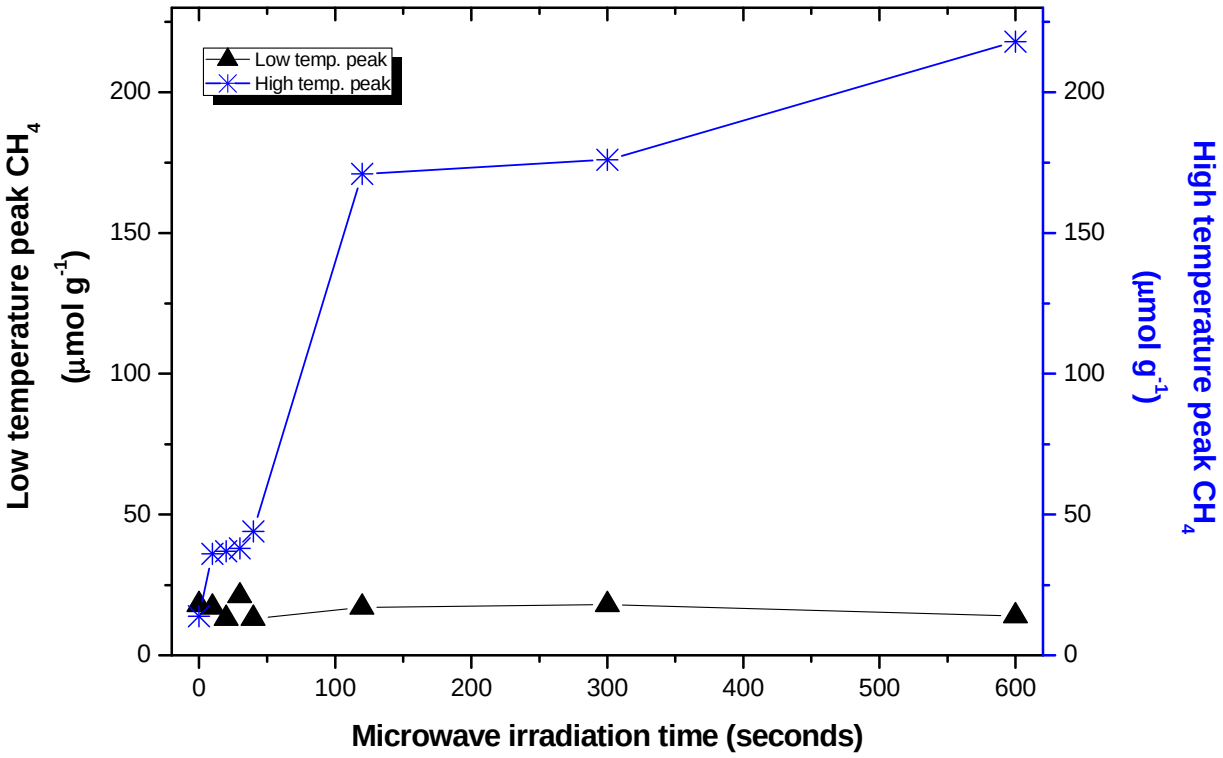



**Figure 5.14** Variations in methane content produced from the low temperature and the high temperature TPSR peaks as a function of the microwave irradiation time. The 1.0K/10Fe/$SiO_2$ catalyst was studied.

### 5.3.5.5 Microwave effect on the catalyst crystallite size: DP vs. IWI

The microwave pre-treatment effect on catalysts with different crystallite sizes was examined by preparing catalysts of the same composition using two techniques; deposition precipitation (DP) and incipient wetness impregnation (IWI). The loading of potassium was maintained at 1 wt. % , while the iron loading was kept at 10 wt. % in both catalysts. The catalyst prepared using the DP procedure is herein referred to as 1.0K/10Fe/$SiO_2$-DP, while the IWI-prepared catalyst was labelled 1.0K/10Fe/$SiO_2$

(results taken from preceding section). As reported in the literature, the iron particles in a catalyst prepared using deposition precipitation have much smaller particle sizes than those prepared using the incipient wetness impregnation technique.[28,29] 1.0K/10Fe/$SiO_2$-DP catalysts had an average particle size in the range 10 – 25 nm, whereas 1.0K/10Fe/$SiO_2$ catalysts had an average particle size in the range 40 – 60 nm.

Changes in the surface properties of these catalysts that were induced by microwave pre-treatment have been studied using the TPSR technique. Peak analysis for these catalysts was done as shown in the preceding section and the profiles were also recorded as a function of the MW irradiation time. A plot of the total $CH_4$ evolved for the two catalysts prepared using these different procedures is shown in Figure 5.15. The data is tabulated in Table 5.8. As expected, the catalyst prepared using the deposition precipitation technique produced more methane relative to its incipient wetness impregnation counterpart for the un-modified catalysts (i.e. at 0 seconds). This is because catalysts prepared using the DP procedure have small crystallites and are hence highly active. As the pre-treatment time was increased to 10 seconds, 2 minutes, 5 minutes and then eventually 10 minutes, the total methane produced is seen to increase from both samples. The DP-prepared catalyst showed lower TPSR activity relative to the IWI-prepared catalyst. This undoubtedly shows that microwave pre-treatment is favoured for larger particle sizes than for smaller ones. As seen in the preceding sections, MW pre-treatment also favours $CH_4$ formation from γ- and δ-carbon species even in these samples.

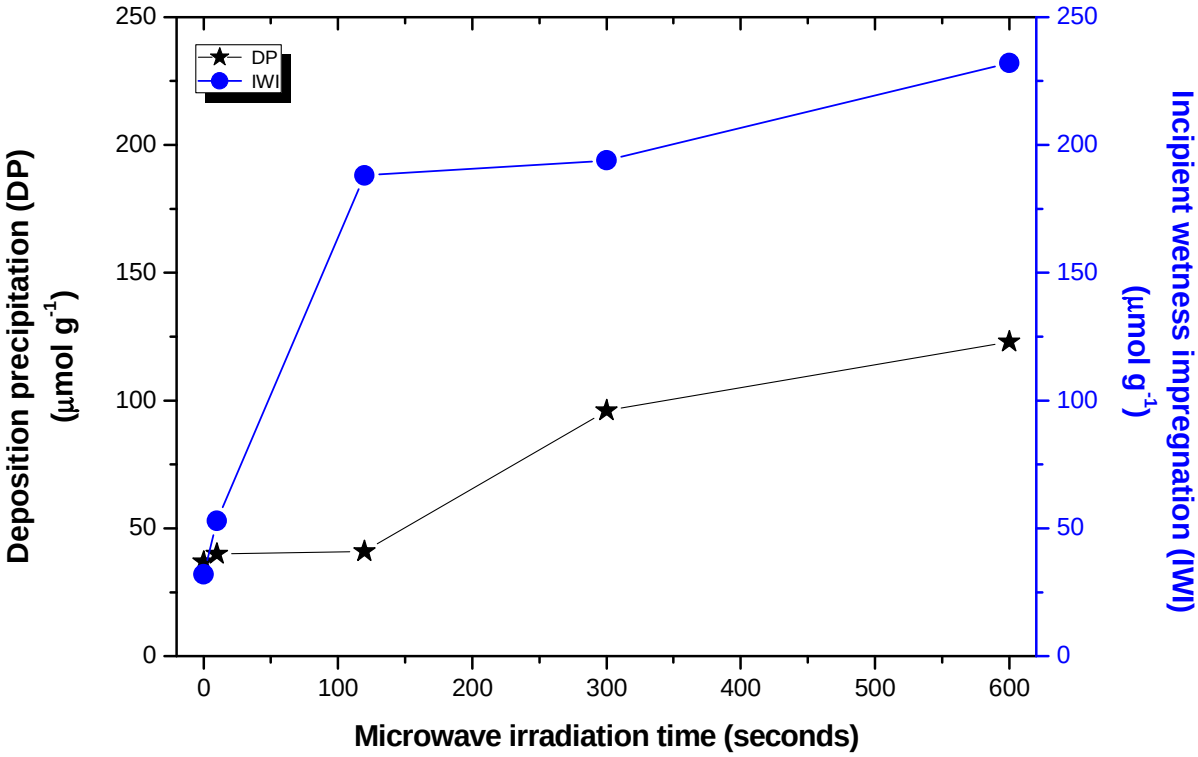



**Figure 5.15** Total $CH_4$ produced in the TPSR by the 1.0K/10Fe/$SiO_2$-DP and the 1.0K/10Fe/$SiO_2$ catalysts that were irradiated for varying periods with microwaves.

**Table 5.8** Total methane produced values that were used to plot Figure 5.15.

| Microwave irradiation time | Total methane evolved (µmol $g^{-1}$) | |
|---|---|---|
| | **DP** | **IWI** |
| **0 seconds** | 37 | 32 |
| **10 seconds** | 40 | 53 |
| **2 minutes** | 41 | 188 |
| **5 minutes** | 96 | 194 |
| **10 minutes** | 123 | 232 |

### 5.3.5.6 Methanator studies

Methanation studies were performed to confirm if microwave pre-treatment had an effect on the strength of CO chemisorption on the surface of the catalyst. The methanator used consisted of a nickel catalyst, and was used to convert CO into $CH_4$. Figure 5.16 shows the methane profiles resulting from TPSR experiments performed *via* a methanator for the catalysts with varying loadings of potassium.

As can be observed in the figure the hydrogenation of adsorbed CO leads to the formation of numerous $CH_4$ peaks. These peaks occur at 115 $^oC$ and 211 $^oC$ for the 0.2 wt. % K sample and extra peaks are observed at higher temperatures for samples with increased potassium loadings. Both the low temperature peaks are attributed to weak CO chemisorption in the molecular state. The low temperature peak at 115 $^oC$ is due to catalytic active sites that are not influenced by the potassium promoter, while the signal at 211 $^oC$ is due to sites that are influenced by the potassium promoter. A similar classification has also been used by Pour *et al.*[30,31] when copper was used to promote an Fe catalyst. In this work these peaks were found to be the biggest when using the 1.5 K/10 $Fe/SiO_2$ catalyst. The low temperature peak is absent at a potassium loading of 1.5 wt. %, indicating that all the catalytic sites responsible for weakly chemisorbed CO at this loading were affected by the potassium promoter. $CH_4$ signals produced from strongly chemisorbed CO shifts to higher temperatures when a methanator is used, appearing at about 521 $^oC$.

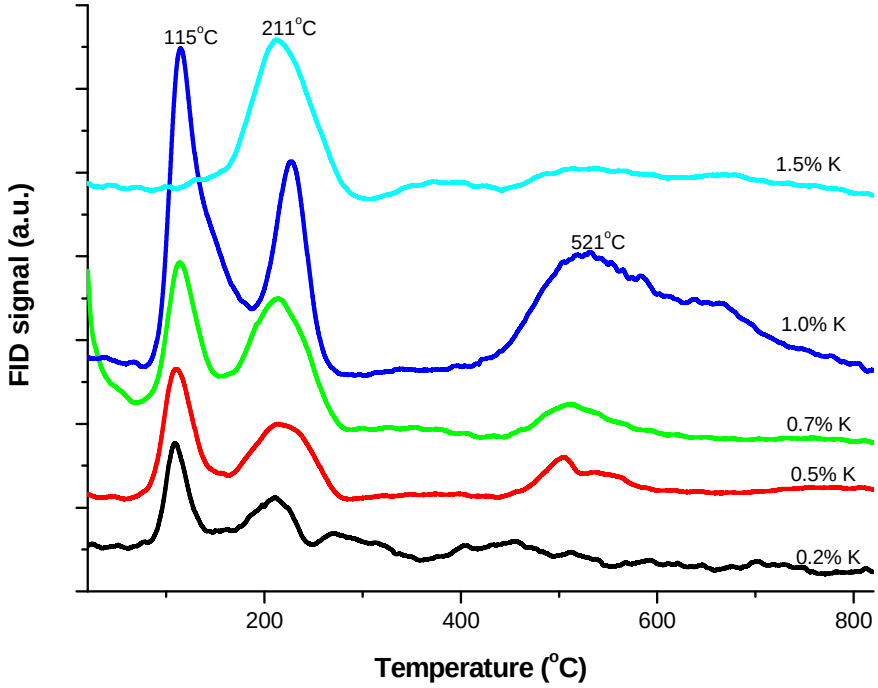



**Figure 5.16** TPSR profiles indicating the effect of potassium on $Fe/SiO_2$ catalysts, prior to microwave pre-treatment. These experiments were performed in a GC fitted with a methanator that utilizes a nickel catalyst.

## 5.3.5.6.1 The effect of microwave pre-treatment

The TPSR profiles illustrated in Figure 5.17 show the formation of methane from $0.7K/10Fe/SiO_2$ and $0.7K/10Fe/SiO_2$-MW catalysts that were analysed *via* the methanator. Table 5.9 compares the integrated peak areas for the three signals obtained from the microwaved and the non-microwaved catalysts. Analysis of data from Peak 1 and Peak 2 from both catalysts showed that there is a slight decrease in $CH_4$ formation from the $0.7K/10Fe/SiO_2$-MW catalyst, whereas these peaks are much bigger for the $0.7K/10Fe/SiO_2$ catalyst. On the other hand the area for Peak 3 is much bigger for the $0.7K/10Fe/SiO_2$-MW than the $0.7K/10Fe/SiO_2$ catalyst. Since this signal is attributed to strongly (dissociatively) chemisorbed CO, it is clear that microwave pre-treatment favours the formation of strong CO chemisorption sites.

Microwave pre-treatment results in a 6% overall increase in methane production at this potassium loading.

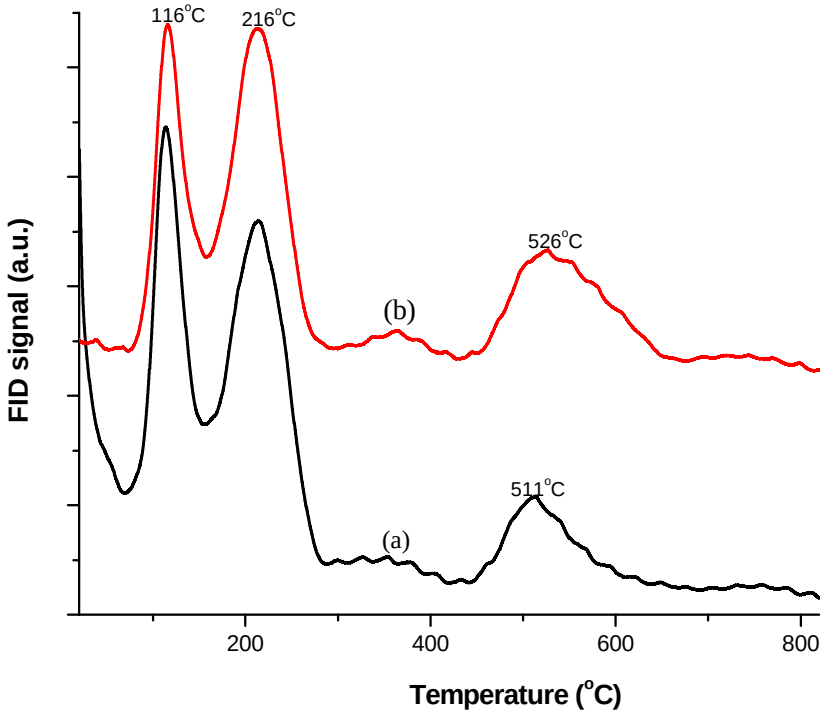



**Figure 5.17** TPSR profiles for the 0.7K/10Fe/$SiO_2$ and 0.7K/10Fe/$SiO_2$-MW catalyst before MW pre-treatment (a) and after 10 seconds of MW pre-treatment (b). Pre-treatment conditions: 450 W, 10 seconds.

**Table 5.9** Peak areas obtained when TPSR is performed *via* the methanator using a 0.7K/10Fe/$SiO_2$ catalyst.

| **Catalyst** | **Peak 1** | **Peak 2** | **Peak 3** | **Total (a.u.)** |
|---|---|---|---|---|
| **0.7K/10Fe/$SiO_2$** | 806 | 1236 | 385 | 2427 |
| **0.7K/10Fe/$SiO_2$-MW** | 704 | 1186 | 678 | 2568 |

The pre-treatment effect was also investigated in catalysts with a 1.0 wt. % potassium loading. Figure 5.18 shows methane profiles for 1.0K/10Fe/$SiO_2$ and 1.0K/10Fe/$SiO_2$-MW done *via* the methanator. The data from these profiles is tabulated in Table 5.10. These catalysts display the microwave effect seen at 0.7 wt. % potassium loading in a more pronounced manner. The signals due to weakly chemisorbed CO (116 $^oC$ and 209 $^oC$) resulted in 2142 and 1303 units of $CH_4$ for the non-microwaved sample, whereas the microwaved sample led to 789 and 1716 peak area units. However, Peak 3 resulted in a larger peak area of 5794 units in the microwaved sample relative to its non-microwaved counterpart (2746 units). This data confirms earlier findings that microwave pre-treatment promotes the formation of strong CO chemisorption sites while suppressing weak CO chemisorption sites in iron catalysts. This could indicate that the MW pre-treatment effect actually increases the binding efficiency of CO on to iron. Microwave pre-treatment resulted in a 34% overall increase in the total $CH_4$ evolved at this potassium loading. It is clear from the profiles that modification of the catalysts using microwave irradiation does affect the production of hydrocarbons and the effect is dependant on the loading of potassium.

**Table 5.10** Peak areas obtained when TPSR is performed *via* the methanator using a 1.0K/10Fe/$SiO_2$ catalyst.

| **Catalyst** | **Peak 1** | **Peak 2** | **Peak 3** | **Total (a.u.)** |
|---|---|---|---|---|
| **1.0K/10Fe/$SiO_2$** | 2142 | 1303 | 2746 | 6191 |
| **1.0K/10Fe/$SiO_2$-MW** | 789 | 1716 | 5794 | 8299 |

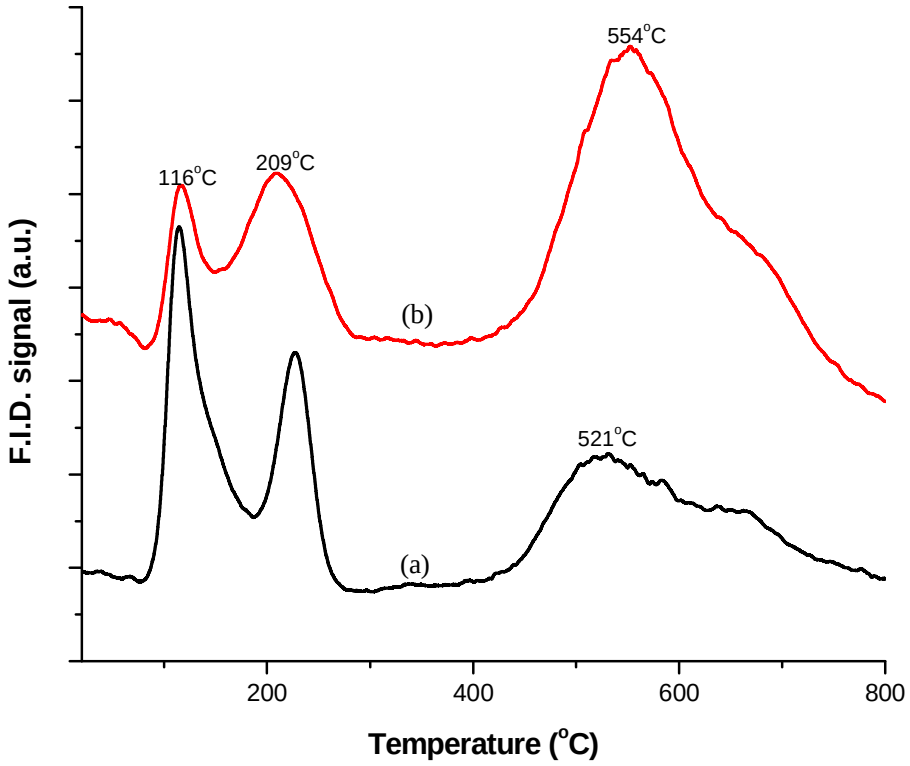



**Figure 5.18** TPSR profiles for the 1.0K/10Fe/$SiO_2$ catalyst (a) before MW pre-treatment and (b) after 10 seconds of MW pre-treatment. Pre-treatment conditions: 450 W, 10 seconds.

## 5.3.6 Fischer Tropsch synthesis (FTS)

### 5.3.6.1 The effect of potassium

The effect of potassium ions on FT activity at a reaction temperature of 275 $^{o}$C was tested in a stainless steel fixed bed reactor. Catalytic activity was measured by computing the carbon monoxide (CO) conversion with respect to time on stream (TOS). The CO conversions with time on stream for the 0.2K/10Fe/$SiO_2$, 0.7K/10Fe/$SiO_2$ and 1.5K/10Fe/$SiO_2$ catalysts are shown in Figure 5.19. The steady state CO conversions for these catalysts are displayed in Figure 5.20. For the samples with potassium loadings of 0.2, 0.7 and 1.5 weight percent, CO conversions of 24.6, 17.8 and 12.4% were obtained at steady state conditions. This data shows that increasing the loading of potassium significantly lowers the CO conversion ability of a catalyst.

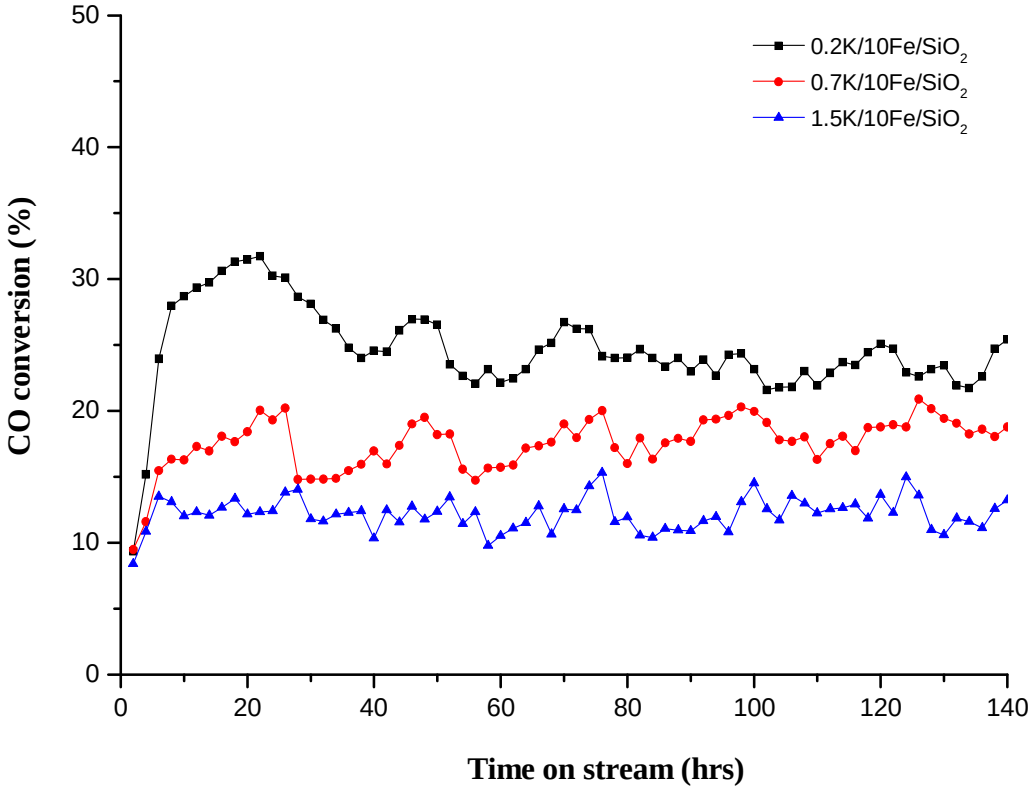



**Figure 5.19** CO conversions for the 0.2K/10Fe/$SiO_2$, 0.7K/10Fe/$SiO_2$ and 1.5K/10Fe/$SiO_2$ catalysts that were not microwaved.

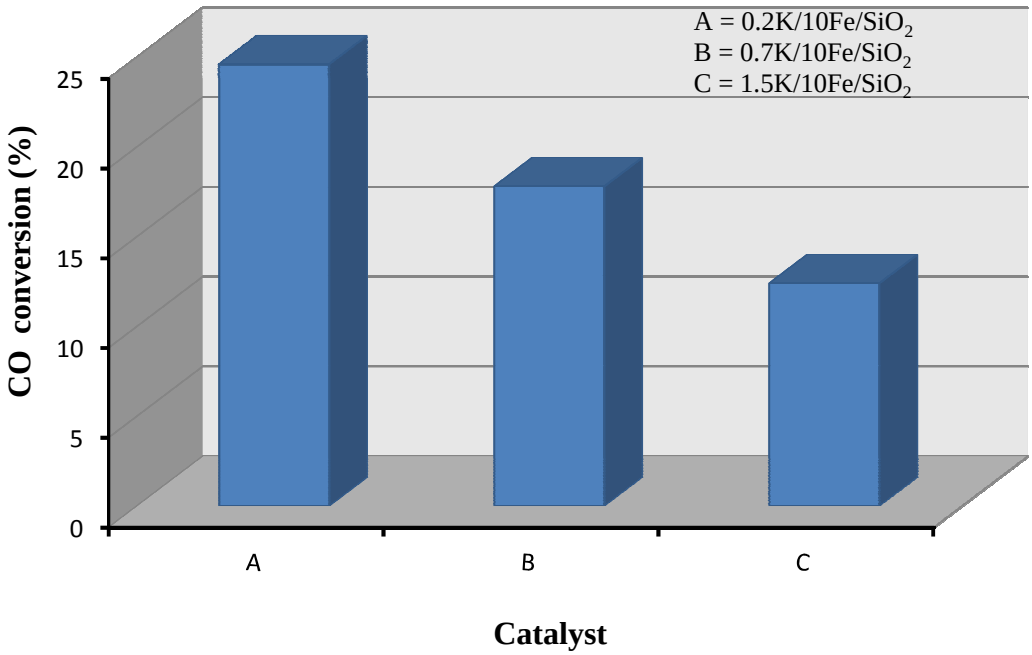



**Figure 5.20** Steady state conversions for the various catalysts before microwave pre-treatment.

Several researchers[32-35] have investigated the effect of potassium on the FTS activity over various iron-based catalysts under different reaction conditions. It has been reported that FTS activity either increases[36] or passes through a maximum as a function of potassium loading[12,27], and potassium either has little effect on the activity for FTS or suppresses it.[27,37] Data obtained in this study indicates that addition of the alkali metal ions suppresses FT activity and this could be explained by various reasons. At high promoter concentrations, the active sites in the catalyst may be covered by potassium, resulting in a decline of the catalyst activity. Dry and Oosthuizen[17] have also reported that carbonization of iron during FTS proceeded more rapidly on potassium promoted catalysts.

Data showing the steady state performances for the catalysts is tabulated in Table 5.11. From the table it is evident that increasing the promoter loading decreases the CO consumption rate, the FT reaction rate and the activity. The activity decreases from 21.4 to 3.96 μmol/sec.gFe as the potassium content is increased from 0.2 to 1.5 wt. %.

Selectivity towards different hydrocarbon fractions was studied using an online GC fitted with an FID and they are reported as percentages. Selectivity towards methane was observed to decline as the promoter content increased. The 1.5K/10Fe/$SiO_2$ catalyst had the highest $C_5$-$C_8$ proportion (44.9 wt. %), followed by the 0.7K/10Fe/$SiO_2$ catalyst (28.0 wt. %). This indicates that as the K/Fe ratio increases, the proportion of methane in the products decreases and the fraction of $C_2$+ products increases. Addition of the alkali metal ions is also seen to increase ethylene selectivity in the $C_2$ hydrocarbons. The increase is from 7.69 to 61.9%. The observed trends were expected and they are consistent with the tendency of the alkali metal ions to decrease the hydrogenation ability of a catalyst and thus accelerate chain growth probability and the olefin selectivity, possibly as a result of the increased basicity.[11] The chain growth probability was seen to increase from 0.55 to 0.79 as the loading of potassium was increased.

**Table 5.11** Effect of potassium content on the catalyst activity and selectivity.

| **Catalyst** | **0.2K/10Fe/$SiO_2$** | **0.7K/10Fe/$SiO_2$** | **1.5K/10Fe/$SiO_2$** |
|---|---|---|---|
| **CO conversion (%)** | 24.6 | 17.8 | 12.4 |
| **Rate CO (mol/s)** | $-5.34 \times 10^{-7}$ | $-3.84 \times 10^{-7}$ | $-9.90 \times 10^{-8}$ |
| **Rate $CO_2$ (WGS)** | $2.08 \times 10^{-7}$ | $1.25 \times 10^{-7}$ | $2.33 \times 10^{-8}$ |
| **Rate FT** | $3.26 \times 10^{-7}$ | $2.59 \times 10^{-7}$ | $7.57 \times 10^{-8}$ |
| **Activity (µmol/sec.gFe)** | 21.4 | 15.4 | 3.96 |
| **α** | 0.55 | 0.59 | 0.79 |
| **$C_2$ olefin %**[a] | 7.69 | 39.3 | 61.9 |
| | | | |
| **Selectivity** | | | |
| **$C_1$** | 28.2 | 14.6 | 3.8 |
| **$C_2 - C_4$** | 38.6 | 42.4 | 36.2 |
| **$C_5 - C_8$** | 18.2 | 28.0 | 44.9 |
| **$CO_2$** | 8.55 | 5.11 | 1.27 |

[a] $C_{2=}/C_2 + C_{2=}$) [Olefin to total $C_2$ hydrocarbon weight ratio]

**Reaction conditions**: $H_2/CO = 2$, flow rate = 20 ml/min, t = 150 h, T = 275 $^oC$, P = 1.0 MPa

### 5.3.6.2 The effect of microwave pre-treatment

The prepared samples were subsequently microwaved to modify their catalytic properties. Microwave modification was performed at 450 W power level for 10 seconds. FTS was performed using a set of pre-defined reaction conditions for all the catalysts (275 $^{o}$C, 1.0 MPa, $H_2$/CO: 2). Figure 5.21 shows the effect of potassium on the CO conversion behaviour for the various microwaved samples. The activity of the catalysts declines from 30.5 to 14.6% as the promoter content is increased from 0.2 to 1.5 wt. %.

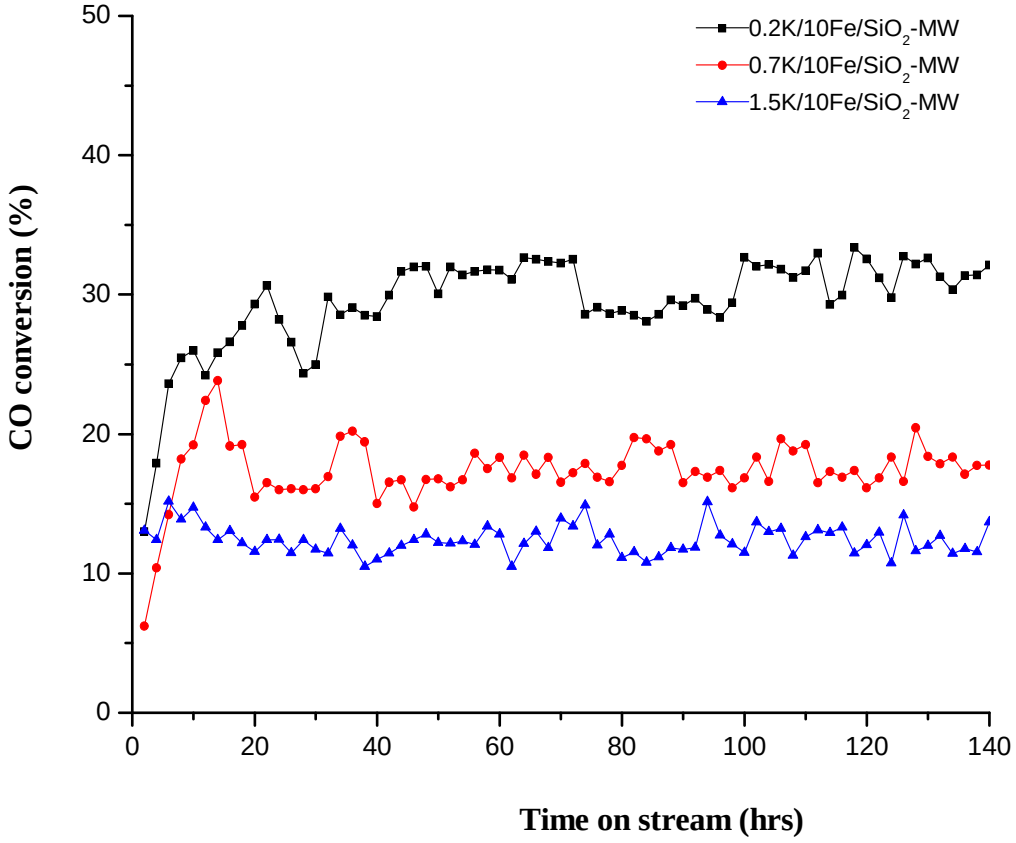



**Figure 5.21** CO conversions for the various microwave pre-treated catalysts. Pre-treatment conditions: 450 W power level, 10 seconds.

Figure 5.22 compares the CO conversions for the corresponding microwaved and non-microwaved samples at steady state. It is evident that both microwaved and non-microwaved samples display a similar trend: as the K/Fe ratio increases, the activity

of the catalyst declines. It was observed, however, that the 0.2K/10Fe/$SiO_2$-MW sample gave a significantly higher CO conversion (30.5%) relative to its non-microwaved counterpart (24.6%). This is attributed to the microwave pre-treatment effect.

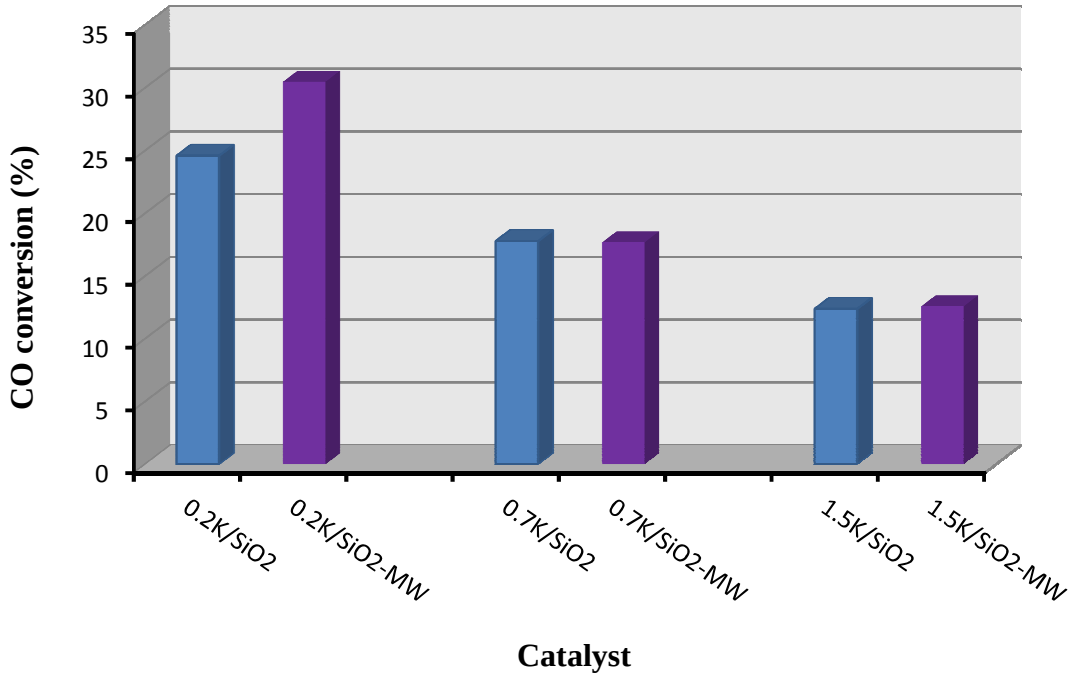



**Figure 5.22** A comparison of CO conversions for microwaved and non-microwaved samples obtained at steady state conditions.

Data comparing the steady state performances of the microwave pre-treated and the non-pre-treated samples is displayed in Table 5.12. Addition of the promoter to the microwaved samples lowers the selectivity towards methane and the low hydrocarbons ($C_2$-$C_4$), while the selectivity towards the heavier hydrocarbons ($C_5$-$C_8$) is enhanced. Analysis of the microwave effect on samples of the same composition indicates that selectivity towards methane is suppressed in the microwave modified catalysts at low potassium loadings (0.2 and 0.7 wt. %). Microwave pre-treatment seems to enhance methane selectivity at high potassium loadings. The modified samples also displayed improved chain growth probabilities at low alkali loadings,

while a slight decrease in the alpha value is observed on the sample with a high potassium loading.

Olefinity was analysed by measuring the $C_2$ olefin proportion relative to the total $C_2$ fraction in the products. Potassium addition clearly favours the formation of olefins for both microwaved and non-microwaved samples. Reasons for this observation are well documented in the literature.[38,39] Comparing catalysts of similar compositions shows that microwave pre-treatment enhances olefin formation for the samples with 0.2 and the 0.7 wt. % potassium. Ethylene content increases from 7.69 to 16.8 wt. % for the 0.2K/10Fe/$SiO_2$-MW catalyst, while for the 0.7K/10Fe/$SiO_2$-MW catalyst the increase is from 39.3 to 41.5 wt. %. The increase in the olefin content is attributed to the effect of microwave pre-treatment, since all other variables were kept constant. The ethylene fraction declines from 61.9 to 55.6 wt. % for the 1.5K/10Fe/$SiO_2$-MW sample. This suggests that microwave modification only enhances olefin formation when low alkali metal loadings (0.2 to 0.7 wt. %) are used. However, the microwave effect suppresses olefin formation at high promoter loadings.

Using iron catalysts instead of cobalt catalysts in FTS promotes the water gas shift (WGS) reaction. $CO_2$ selectivity is normally used as a measure of the WGS activity. When making the calculations, all the $CO_2$ produced during FTS is assumed to be produced by the WGS reaction. Selectivity towards $CO_2$ was noted to decline relatively at low promoter loadings while it was enhanced in the sample with the highest potassium content. A decline in the WGS reaction is undesirable since it results in excess water in the reactor. Excess water promotes the deactivation of the catalyst.

**Table 5.12** Effect of potassium content and microwave pre-treatment on catalyst activity and selectivity.

| **Catalyst**[a] | **0.2K/$SiO_2$** | **0.2K/$SiO_2$-MW** | **0.7K/$SiO_2$** | **0.7K/$SiO_2$-MW** | **1.5K/$SiO_2$** | **1.5K/$SiO_2$-MW** |
|---|---|---|---|---|---|---|
| **CO conversion (%)** | 24.6 | 30.5 | 17.8 | 17.7 | 12.4 | 14.6 |
| **Rate CO (mol/s)** | $-5.34 \times 10^{-7}$ | $-3.71 \times 10^{-7}$ | $-3.84 \times 10^{-7}$ | $-3.50 \times 10^{-7}$ | $-9.90 \times 10^{-8}$ | $-2.13 \times 10^{-7}$ |
| **Rate $CO_2$ (WGS)** | $2.08 \times 10^{-7}$ | $1.16 \times 10^{-7}$ | $1.25 \times 10^{-7}$ | $1.16 \times 10^{-7}$ | $2.33 \times 10^{-8}$ | $7.34 \times 10^{-8}$ |
| **Rate FT** | $3.26 \times 10^{-7}$ | $2.55 \times 10^{-7}$ | $2.59 \times 10^{-7}$ | $2.34 \times 10^{-7}$ | $7.57 \times 10^{-8}$ | $1.39 \times 10^{-7}$ |
| **Activity (µmol/sec.gFe)** | 21.4 | 14.8 | 15.4 | 14.0 | 3.96 | 8.50 |
| **α** | 0.55 | 0.56 | 0.59 | 0.66 | 0.79 | 0.77 |
| **$C_2$ olefin %**[b] | 7.69 | 16.8 | 39.3 | 41.5 | 61.9 | 55.6 |
| **Selectivity** | | | | | | |
| **$C_1$** | 28.2 | 26.2 | 14.6 | 11.4 | 3.8 | 12.4 |
| **$C_2 – C_4$** | 38.6 | 39.9 | 42.4 | 38.3 | 36.2 | 35.8 |
| **$C_5 – C_8$** | 18.2 | 18.9 | 28.0 | 35.3 | 44.9 | 36.7 |
| **$CO_2$** | 8.55 | 4.77 | 5.11 | 4.74 | 1.27 | 3.09 |

[a] All the catalysts contained 10 wt. % Fe

[b] $C_{2=}/(C_2 + C_{2=})$ [Olefin to total $C_2$ hydrocarbon weight ratio

Maximum error is ± 5%

**Catalyst mass:** 0.5 g

**Reaction conditions:** H2/CO = 2, flow rate = 20 ml/min, t = 150 h, T = 275 $^oC$, P = 1.0 MPa

### 5.3.6.3 Effect of the MW irradiation time

In the preceding section, it has been shown that the 1.5K/10Fe/$SiO_2$-MW catalyst had the largest improvement in activity (3.96 to 8.5 μmol/sec.gFe) which was induced by microwave modification of the catalyst. Of course, it was desirable to understand why this was the case. The microwave irradiation time of the sample was consequently increased from 10 seconds to 10 minutes but the power level was maintained at 450 W. The FT data obtained is compared in Table 5.13. It is evident from the table that increasing the microwave exposure time does not have a significant influence on CO conversion. The CO conversion was 12.4% for both the non-microwaved and the microwaved (10 minutes) samples.

**Table 5.13** The effect of the MW irradiation time on FT activity and selectivity

| **Catalyst** | **1.5K/$SiO_2$** | **1.5K/$SiO_2$-MW (10 seconds)** | **1.5K/$SiO_2$-MW (10 minutes)** |
|---|---|---|---|
| **CO conversion (%)** | 12.4 | 14.6 | 12.4 |
| **Rate CO (mol/s)** | -9.90 x 10-8 | -2.13 x 10-7 | -2.25 x 10-7 |
| **Rate $CO_2$ (WGS)** | 2.33 x 10-8 | 7.34 x 10-8 | 5.46 x 10-8 |
| **Rate FT** | 7.57 x 10-8 | 1.39 x 10-7 | 1.70 x 10-7 |
| **Activity (μmol/sec.gFe)** | 3.96 | 8.50 | 8.99 |
| **α** | 0.79 | 0.77 | 0.63 |
| **$C_2$ olefin %**[a] | 61.9 | 55.6 | 67.0 |
| | | | |
| **Selectivity** | | | |
| **$C_1$** | 3.8 | 12.4 | 9.33 |
| **$C_2 – C_4$** | 36.2 | 35.8 | 39.3 |
| **$C_5 – C_8$** | 44.9 | 36.7 | 36.3 |
| **$CO_2$** | 1.27 | 3.09 | 2.25 |

Further increase of the microwave exposure time only had a slight effect on the activity as it increased from 8.50 to 8.99 μmol/sec.gFe after 10 minutes. Nonetheless pre-treatment clearly

improved the activity of the catalyst because the non-microwaved sample had an activity of 3.96 μmol/sec.gFe. Hydrocarbon selectivities were also affected by the longer duration of microwave exposure. Increasing the microwave irradiation period was noted to increase methane selectivity and thus lower the formation of higher hydrocarbons. Consequently, the alpha value dropped from 79 to 63% as the irradiation period was increased to 10 minutes.

Even though the percentage CO conversions are similar, the rate of CO consumption increases from $-9.90 \times 10^{-8}$ to $-2.25 \times 10^{-7}$ mol/s as the irradiation time increases. This is justified by the considerably high $CO_2$ levels produced from the samples that were irradiated for 10 seconds and 10 minutes. This is desirable as it suggests that the WGS reaction is enhanced. Data on the rate of $CO_2$ production (WGS) confirms this observation. As shown in Table 5.15 ethylene selectivity was also enhanced by increasing the duration of the pre-treatment period.

It was observed that certain parameters like the ethylene and $CO_2$ selectivities were enhanced by microwave pre-treatment (10 seconds) at low alkali ion concentration. These parameters were suppressed by high alkali ion concentration on the surface of the metal if pre-treatment was performed for 10 seconds. However if the irradiation period is increased, even at high promoter loadings these parameters do improve. It was also noted that certain parameters like the FT reaction rate and the activity declined as a result of having excess potassium on the surface of the catalyst. However, pre-treatment improved both the FT reaction rate and the activity. It is therefore believed that microwave pre-treatment can enhance FT performance at all potassium loadings, but different loadings require different irradiation times.

## *5.4 Conclusions*

The aim of this chapter was to determine the effect of potassium in silica supported catalysts that were pre-treated using microwave radiation. The potassium weight loading was varied within the range 0–1.5 wt. %. As with the unsupported catalysts, microwave pre-treatment was found not to induce any modifications on the bulk properties of these catalysts.

Microwave solid-state modification of the catalysts had a significant impact on the CO adsorption characteristics of these catalysts. While the effect of potassium was relatively insignificant in non-pre-treated catalysts on the TPSR-MS, the effect was huge in microwave modified catalysts. Microwave pre-treatment induced an overall increase of 13% in $CH_4$ formation for a 0.2 wt. % K catalyst, and this continued to rise with the potassium loading up to a 1.0 wt. % K catalyst where an increase of 65% in $CH_4$ evolution was recorded. Microwaves were found to promote $CH_4$ formation from 'graphitic' carbon in these catalysts, while decreasing $CH_4$ formation from α- and β-carbon species. CO adsorption investigations done *via* a methanator also showed that microwave pre-treatment favoured strong CO adsorption while suppressing weak CO adsorption. This indicated that the binding of CO to iron is enhanced in microwave modified catalysts.

The microwave effect was seen to increase drastically in these silica-supported catalysts as the irradiation time was increased from 10 seconds to up to 10 minutes. Comparing catalysts with small and large crystallites of the same loading of potassium showed that the microwave effect is amplified in catalysts with larger particles compared to smaller crystallites.

FTS performance was also improved by microwave modification. At low alkali concentration, microwaved samples showed improved ethylene selectivities, higher alpha values and low methane and $C_2$-$C_4$ selectivities. For the 0.7K/10Fe/$SiO_2$ catalyst, the alpha value improved from 0.59 to 0.66 due to microwave pre-treatment. Microwave modification of catalysts with high alkali loadings resulted in a decline in the chain growth probability, olefin selectivity and also improved methane selectivity.

## *5.5 References*


(1) Fischer, F.; Tropsch, H. *Brennst.-Chem.* **1923**, *4*, 276.

(2) Fischer, F.; Tropsch, H. *Brennst.-Chem.* **1926**, *7*, 97.

(3) Rao, V. S.; Stiegel, G. J.; Cinquergrane, G. J.; Srivastava, R. D. *Fuel Process. Technol.* **1992**, *30*, 83.

(4) Jin, Y.; Datye, A. K. *J. Catal.* **2000**, *196*, 8.

(5) Shroff, M. D.; Kalakkad, D. S.; Coulter, K. E.; Kohler, S. D.; Harrington, M. S.; Jackson, N. B.; Sault, A. G.; Datye, A. K. *J. Catal.* **1995**, *156*, 185.

(6) O'Brien, R. J.; Xu, L.; Bao, S.; Raje, A. P.; Davis, B. H. *Appl. Catal. A: Gen.* **2000**, *196*, 173.

(7) Jackson, N. B.; Datye, A. K.; Mansker, L.; O'Brien, R. J.; Davis, B. H. In *Studies in surface science and catalysis*; Bartholomew, C. H., Fuentes, G. A., Eds.; Elsevier Science: Amsterdam, 1997; Vol. 136, p 63.

(8) Zhao, R.; Goodwin, J. G.; Jothimurugesan, K.; Gangwal, S. K.; Spivey, J. J. *Ind. Eng. Chem. Res.* **2001**, *40*, 1320.

(9) Pham, H. N.; Nowicki, L.; Xu, J.; Datye, A. K.; Bukur, D. B.; Bartholomew, C. H. *Ind. Eng. Chem. Res.* **2003**, *42*, 4001.

(10) Kalakkad, D. S.; Shroff, M. D.; Kohler, S. D.; Jackson, N. B.; Datye, A. K. *Appl. Catal. A: Gen.* **1995**, *133*, 335.

(11) Zhang, Q.; Kang, J.; Wang, Y. *Chem. Cat. Chem.* **2010**, *2*, 1030.

(12) Dry, M. E. *The Fischer-Tropsch Synthesis, in Catalysis Science and Technology*; Springer-Verlag: New York, 1981; Vol. 159.

(13) Yang, Y.; Xiang, H.; Tian, L.; Wang, H.; Zhang, C.; Tao, Z.; Xu, Y.; Zhong, B.; Li, Y. *Appl. Catal. A: Gen.* **2005**, *284*, 105.

(14) Dlamini, H.; Motjope, T.; Joorst, G.; ter Stege, G.; Mdleleni, M. *Catal. Lett.* **2002**, *78*, 201.

(15) Anderson, R. B. *The Fischer-Tropsch Synthesis*; Academic Press: New York, 1984.

(16) Mokoena, E. M. Ph.D. thesis, University of the Witwatersrand, 2005.

(17) Dry, M. E.; Oosthuizen, G. J. *J. Catal.* **1968**, *11*, 18.

(18) Leith, I. R.; Howden, M. G. *Appl. Catal. A: Gen.* **1988**, *37*, 75.

(19) Yang, Y.; Xiang, H.; Xu, Y.; Bai, L.; Li, Y. *Appl. Catal. A: Gen.* **2004**, *266*, 181.

(20) Stobe, D. E.; van Buren, F. R.; van Dillen, A. J.; Geus, J. W. *J. Catal.* **1992**, *135*, 533.

(21) Guglielminotti, E.; Boccuzzi, F.; Pinna, F.; Strukul, G. *J. Catal.* **1997**, *167*, 153.

(22) Dry, M. E.; Shingles, T.; Boshoff, L. J.; Oosthuizen, G. J. *J. Catal.* **1969**, *15*, 190.

(23) Graf, B.; Muhler, M. *Phys. Chem. Chem. Phys.* **2011**, *13*, 3701.

(24) Xu, J.; Bartholomew, C. H. *J. Phys. Chem. B.* **2005**, *109*, 2392.

(25) Zhang, C.; Zhao, G.; Liu, K.; Yang, Y.; Xiang, H.; Li, Y. *J. Mol. Catal. A: Chem.* **2010**, *328*, 35.

(26) Linganiso, L. Z. PhD. Thesis, University of the Witwatersrand, 2008.

(27) Miller, D. G.; Moskovits, M. *J. Phys. Chem.* **1988**, *92*, 6081.

(28) van Steen, E.; Prinsloo, F. F. *Catal. Today* **2002**, *71*, 327.

(29) Lohitharn, N.; Goodwin, J. G. *J. Catal.* **2008**, *260*, 7.

(30) Pour, A. N.; Shahri, S. M. K.; Bozorgzadeh, H. R.; Zamani, Y.; Tavasoli, A.; Marvast, M. A. *Appl. Catal. A: Gen.* **2008**, *348*, 201.

(31) Pour, A. N.; Housaindokht, M. R.; Tayyari, S. F.; Zarkesh, J. *J. Natur. Gas Chem.* **2010**, *19*, 284.

(32) Anderson, R. B.; Seligman, B.; Schultz, J. F.; Elliot, M. A. *Ind. Eng. Chem.* **1952**, *22*, 97.

(33) Kölbel, H.; Giehring, H. *Brennst.-Chem.* **1963**, *44*, 343.

(34) Arakawa, H.; Bell, A. T. *Ind. Eng. Chem. Process. Des. Dev.* **1983**, *22*, 97.

(35) Rankin, J. L.; Bartholomew, C. H. *J. Catal.* **1986**, *100*, 533.

(36) Bukur, D. B.; Mukesh, D. S.; Patal, A. *Ind. Eng. Chem. Res.* **1990**, *29*, 194.

(37) Dictor, R. A.; Bell, A. T. *J. Catal.* **1986**, *97*, 121.

(38) Jiang, M.; Koizumi, N.; Yamada, M. *Appl. Catal. A: Gen.* **2000**, *204*, 58.

(39) Soled, S.; Iglesia, E.; Miseo, S.; DeRites, B. A.; Fiato, R. A. *Top. Catal.* **1995**, *2*, 193.